Alma Mater Studiorum – Università di Bologna

DOTTORATO DI RICERCA IN

BIOLOGIA CELLULARE E MOLECOLARE

Ciclo XXIX

Settore Concorsuale SSC 05/E2

Settore Disciplinare SSD BIO/11

Titolo tesi:

"Approaches to new generation vaccines against pertussis and identification of new virulence factors"

Presentata da:

Gianmarco Gasperini

Relatore:

Prof. Vincenzo Scarlato

Coordinatore Dottorato

Prof. Giovanni Capranico

Correlatore:

Dott.ssa Beatrice Aricò

Esame finale anno 2017

Because getting your dreams
it's strange, but it seems
a little - well - complicated.
There's a kind of a sort of cost,
there's a couple of things that get lost,
There are bridges you cross
you didn't know you crossed
until you've crossed

Fundings

This study was sponsored by GSK Vaccines (formerly Novartis Vaccines).

Table of contents

1. Introduction

1.1. Pertussis disease

Pertussis is a highly contagious, acute respiratory disease whose etiological agent is the Gram-negative bacterium *Bordetella pertussis.* The name pertussis takes its origins from Latin (*per,* intensive, and *tussis,* cough) and describes the most consistent and prominent clinical feature of the illness. The common name for the illness, "whooping cough", comes from the characteristic inspiratory sound made at the end of an episode of paroxysmal coughing.

B. pertussis infection results in colonization and rapid multiplication of the bacteria on the mucous membrane of the respiratory tract. Histopathological studies of fatal pertussis cases documented large airway disease as the principal component of *B. pertussis* infection and showed large numbers of bacteria on cilia lining trachea and bronchi, causing local damage (Mallory and Hornor 1912). More recently, electron microscopy studies have demonstrated that *B. pertussis* adheres exclusively to the tufts of ciliated epithelial cells of the upper respiratory tract; no attachment to non-ciliated cells was observed (Tuomanen and Hendley 1983).

Transmission

B. pertussis is a strict human pathogen and no other animal or environmental reservoir is known. It is transmitted from human to human through aerosolized respiratory droplets expelled via coughing and sneezing, as further demonstrated in a recent study in a baboon model (Warfel, Beren et al. 2012). Adults, who often lack classic symptoms, have a primary role in the spread of the disease, as they serve as important

reservoirs of *B. pertussis*, transmitting pertussis to infants and children, who are at greater risk for morbidity and mortality (Bisgard, Pascual et al. 2004, Wendelboe, Njamkepo et al. 2007).

Clinical manifestations

Clinical manifestations of the infection may show substantial variation, depending on several factors, such as clinical condition and age of the patient, previous vaccination or infection, presence of passively acquired antibodies (Mattoo and Cherry 2005). Pertussis can result in asymptomatic infection, mild cough illness or classic illness. Classic illness often occurs in primary infection in unimmunized children between 1 and 10 years of age (Cherry 1999), lasts 6 to 12 weeks or longer and is divided into three stages: *catarrhal*, *paroxysmal* and *convalescent phase* (Fig.1). After an incubation period of 7 to 10 days, illness begins with the *catarrhal phase*, which lasts 1-2 weeks and is usually characterized by nonspecific symptoms including rhinorrhea, lacrimation, progressive cough, reduced activity, loss of appetite and occasional low-grade fever. At the end of this phase, most children have frequently a leukocytosis with absolute lymphocytosis, which is absent in adults (Postels-Multani, Schmitt et al. 1995, Mattoo and Cherry 2005, Melvin, Scheller et al. 2014). During the subsequent *paroxysmal stage*, lasting 1-6 weeks or longer, the cough becomes more persistent and severe, with paroxysms, consisting of repetitive series of forceful coughs during a single expiration. A paroxysm is often followed by a forced inspiration during which the characteristic whoop occurs and is often associated with tenacious mucus, cyanosis and post-tussive vomiting. The patient usually shows normal airway function between attacks. Infants under 6 months of age may not have the strength to have a whoop, so the disease may manifest with spells of apnea, with consequent bradycardia, cyanosis and unresponsiveness (Christie and Baltimore 1989). The transition to the last *convalescent*

phase is associated with a gradual decrease in the frequency and in the severity of the paroxysms before the patient returns to normal. This stage usually lasts 2-3 weeks but it is often prolonged. Most of the asymptomatic infections or mild illnesses occur in previously immunized or infected subjects, both adolescents and adults. The predominant symptom may be a persistent cough, that is often associated with nonspecific symptoms of more common viral upper respiratory tract infections (Cornia, Hersh et al. 2010). Pertussis is most severe in young infants, but it occurs in all age groups. Most deaths due to pertussis occur in infants, for which the infection is particularly severe: in neonatal infection the risk of death correlates with frequent episodes of apnea, often resulting in seizures due to hypoxia (Christie and Baltimore 1989), whereas in young infants is related directly with lymphocytosis, which positively correlates with intractable pulmonary hypertension, respiratory failure and death (Paddock, Sanden et al. 2008).

1.1.1. *Bordetella pertussis*

Bordetella pertussis was first isolated in pure culture by Bordet and Gengou in 1906. It is a small (approximately 0.5 x 1 μm) encapsulated bacterium, strict aerobe, non-motile and non-sporulating.

Following the inhalation of infected aerosol, *B. pertussis* enters the upper respiratory tract and adheres to ciliated epithelial cells in the nasopharynx and trachea. Once attached to the mucosal surface, *B. pertussis* produces a wide array of virulence factors, including adhesins and toxins. The concerted expression of these factors prevents rapid clearance of the bacteria and enables replication and dissemination to the lower areas of the respiratory tract (de Gouw, Diavatopoulos et al. 2011).

The expression of the majority of these virulence factors is under the control of a two-component regulatory system encoded by the *bvgAS* locus (Arico, Miller et al. 1989). BvgS is a 135-kDa transmembrane sensor kinase consisting of several domains involved in phosphorylation cascade, while BvgA is a 23-kDa response regulator protein, with a receiver domain at its N-terminus and a DNA-binding domain at its C-terminus (Cotter and Jones 2003). Under inducing signals BvgS autophosphorilates and initiate a phopshorelay that leads to BvgA phosphorylation and activation (Uhl and Miller 1996). Activated BvgA dimerizes and binds to specific DNA sequences to positively or negatively regulate transcription (Decker, James et al. 2012). In response to environmental conditions, BvgAS controls the expression of at least three distinct phenotypic phases, each characterized by maximal expression of some genes and minimal expression of others (Lacey 1960). The signals to which BvgS responds *in vivo* are still unknown. Bvg+ phase occurs when bacteria are grown under permissive conditions. In this phase BvgAS is active and promotes the expression of virulence-activated genes (*vag*-genes, divided in class 1 and class 2 genes), while represses the expression of virulence-repressed genes (*vrg*-genes, or class 4 genes) by the repressor protein BvgR, whose gene is located downstream of the *bvgAS* locus and is activated by BvgA (Merkel, Barros et al. 1998). *Vag*-genes encode adhesins and toxins that play a key role in the respiratory tract colonization *in vivo* (Merkel, Stibitz et al. 1998). Bvg-phase occurs when bacteria are grown under modulating conditions, such as growing at low temperature (25°C) or in the presence of nicotinic acid or $MgSO_4$ (Melton and Weiss 1993). During this phase, BvgAS is inactive and is unable to repress *vrg*-genes, which are therefore maximally expressed, while no expression of *vag*-genes occurs. Since these genes are expressed when bacteria are grown under limiting conditions, they may be involved in *B. pertussis* survival in the *ex vivo* environment. Bvg^i phase occurs when bacteria are grown under submodulating conditions (low concentration of

chemical modulators). In this phase bacteria display a phenotype that is intermediate between Bvg+ phase and Bvg- phase, since BvgAS is partially active: *vrg*-genes and class 1 genes (e.g. PT, ACT) are not expressed, while class 2 genes (e.g. FHA) and the genes specific of this phase (class 3 genes) are maximally expressed (Deora, Bootsma et al. 2001). This phenotype may be important for transmission between hosts, but this remains to be elucidated. The complexity of this system may allow multiple levels of control of gene expression that could be important in the infection cycle.

B. pertussis virulence factors include several adhesins and toxins that contribute to its ability to cause the disease. The major virulence factors and antigenic components expessed during the virulent Bvg+ phase, are schematically reported in Table 1 and Fig. 1. Among them, Filamentous hemagglutinin, Pertactin and Pertussis Toxin, are the antigens included in three-component acellular pertussis vaccine.

Virulence Determinant	Description
Filamentous hemagglutinin (FHA)	220 kDa surface-associated and secreted protein. Dominant adhesin, promotes attachment to respiratory epithelium. Immunomodulatory properties.
Pertactin (PRN)	69 kDa outer membrane protein. Autotransporter. Mediates eukaryotic cells binding *in vitro*. Role in resistance to neutrophil-mediated clearance.
Fimbriae (FIM)	Filamentous cell surface structures. Two serologic types (type 2 and 3). Role in mediating adherence to ciliated respiratory epithelium. Potential immunomodulatory activity.
Pertussis toxin (PT)	105 kDa ADP-ribosylating A-B toxin. Responsible of pertussis-associated leukocytosis with lymphocytosis, hypoglycemia and sensitization to histamine. Important immunomodulatory activity. Strong adjuvant.
Adenylate cyclase toxin (ACT)	Calmodulin-activated toxin with adenylate cyclase and hemolysin activity. Anti-inflammatory and antiphagocytic factor. Possible contribution to local tissue damage in the respiratory tract.
Dermonecrotic toxin (DNT)	160 kDa heat-labile cytoplasmic toxin. Activates Rho. Induces necrosis *in vivo* and *in vitro*. Possible role in bacterial survival and local tissue damage in the respiratory tract.
Tracheal cytotoxin (TCT)	921 Da disaccharide-tetrapeptide monomer of peptidoglycan. Not regulated by BvgAS. Causes disruption of tight junctions, damage to cilia with ciliary stasis, IL-1 and NO production.
LOS	Envelope toxin. Often referred to as lipooligosaccharide (LOS) because it lacks O-antigen. Endotoxin activities. Role in antibiotic and serum resistance. Cause of whole cell vaccines reactogenicity.
Type III secretion system (T3SS)	Translocate effector proteins into host cells. Required for persistent tracheal colonization. Immunomodulatory activity. Activates ERK1/2.
Autotransporters (BrkA, TcfA, Vag8, SphB1)	Surface-associated or secreted. Putative roles in mediating adherence, serum resistance, evasion of antibody-mediated clearance, proteolytic processing of other surface proteins.

Table 1. *B. pertussis* main virulence determinants. Adapted from (Mattoo and Cherry 2005)

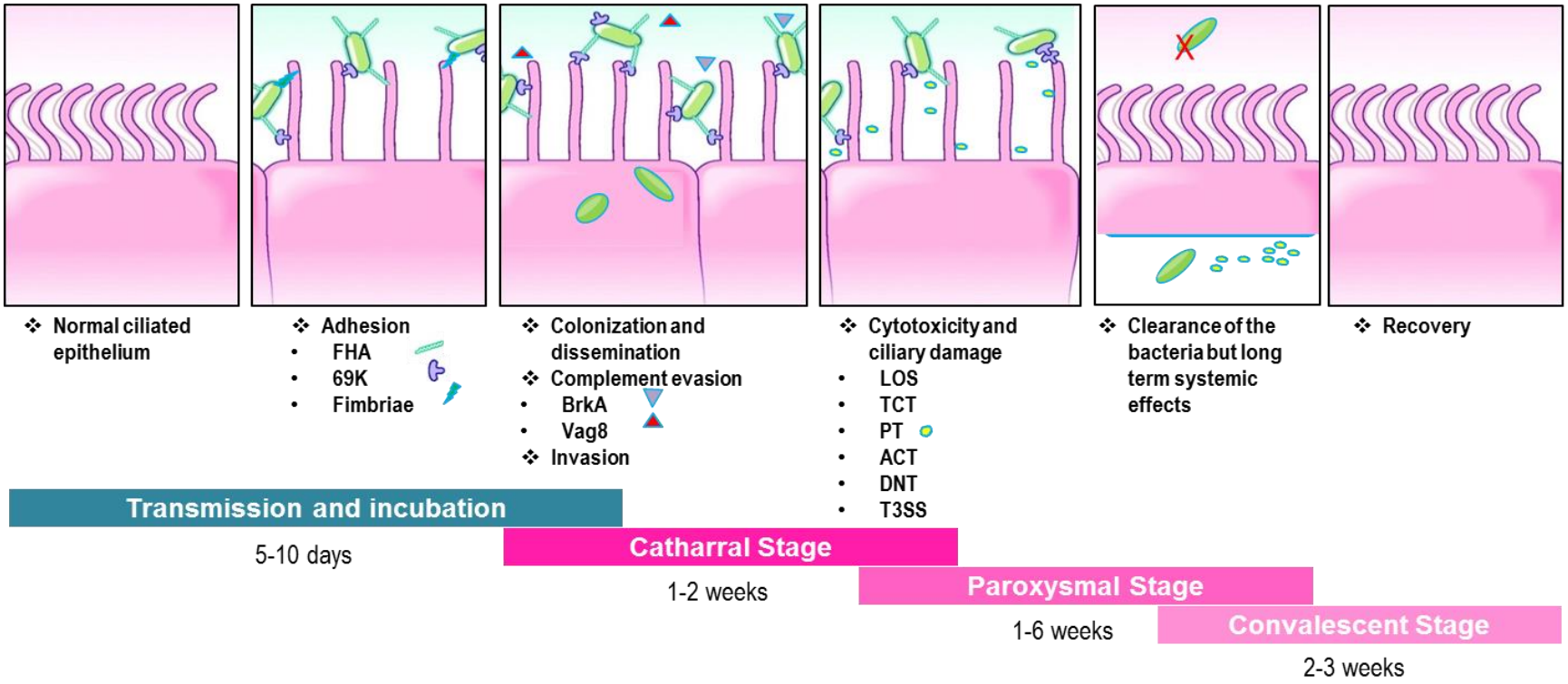

FIG. 1. *B. pertussis* pathogenesis: transmission and disease progression Adapted from (Tozzi, Celentano et al. 2005). *Bordetella pertussis* engages multiple strategies in order to create a niche for colonization of the mucosal epithelium. From left to the right: several virulence factors mediate adhesion to respiratory cells (FHA, 69K, Fimbriae), colonization and dissemination. Bordetella pertussis evades the immune system and the complement mediated killing (BrkA and Vag8) and invades epithelial cells. Tracheal cytotoxin (TCT) and lipo-oligosaccharide (LOS) synergistically evoke ciliary damage to the respiratory epithelium. Pertussis Toxin (PT), Adenylate cyclase toxin (ACT) and the type III secretion system (T3SS) subvert intraepithelial signaling pathways leading to cytotoxicity.

1.1.2. Pertussis vaccines and resurgence of pertussis

In the pre-vaccine era, pertussis was an endemic and epidemic disease mainly affecting young children, with high morbidity and mortality (Cherry 1999). Given the severity of the disease, vaccines were introduced soon after the isolation of the etiological agent, to treat and prevent the disease. Whole-cell pertussis (wP) vaccines, that consist of suspensions of killed *B. pertussis* organisms (Xing, Markey et al. 2014), were first introduced in the 1940s and mass vaccination programs resulted in a rapid reduction in both the incidence of pertussis and the number of death caused by the infection in all age groups. However, the high reactogenicity of wP vaccines due to the presence of endotoxin, including an elevated risk of fever (Barkin and Pichichero 1979) and rare cases of convulsions, motivated the development in the 1980s of acellular pertussis (aP) vaccines. aP vaccines, consisting of one to five purified antigens (PT, FHA, PRN and FIM 2/3), are less reactogenic, thanks to the removal of the LPS, and starting from the late 1990s progressively replaced wP vaccines in many developed countries. Since then, in the last three decades a steady increase in the number of pertussis cases was observed in various countries following aP vaccination programs (Black, Cousens et al. 2010, Chiappini, Stival et al. 2013, Ausiello and Cassone 2014, Mills, Ross et al. 2014), confirming a reemergence of pertussis.

There are several causes that may contribute to the resurgence of pertussis; one of these is the emergence of *B. pertussis* strains that have undergone variations in the antigens included in the vaccine, as consequence of immune selective pressure. Indeed, it has been reported in the past decade the appearance of *B. pertussis* strains with increased production of pertussis toxin and strains pertactin-deficient (de Gouw, Hermans et al. 2014, Mooi, Van Der Maas et al. 2014). Antigenic divergence could affect both

memory recall and the efficacy of antibodies, while higher levels of pertussis toxin may increase suppression of the innate and acquired immune system.

A second possible reason is the waning immunity. Although initially induced at a sufficiently protective level, the acquired pertussis-specific immunity is progressively lost with time. Estimates indicate that infection-acquired immunity against pertussis disease wanes after 4–20 years and protective immunity after vaccination with wP or aP vaccines wanes after 4–12 years. (Wendelboe, Van Rie et al. 2005, Klein, Bartlett et al. 2012). There is also evidence that some wP vaccines induce longer lasting immunity than aP vaccines (Mooi, Van Der Maas et al. 2014). Further research into the rate of waning of vaccine-acquired immunity will help to determine the optimal timing and frequency of booster immunizations and their role in pertussis control.

Another explanation for the increasing incidence of pertussis related to the switch to aP vaccines lies in the difference between the mechanisms of both humoral and cellular immunity induced by natural infection or vaccination with a wP vaccine versus the vaccination with aP vaccine. Studies in murine models have shown that innate immune response help to control bacterial infection, while the complete clearance of bacteria requires cellular immunity mediated by T cells that secrete IFN- γ (T-helper type 1, Th1) and IL-17 (T-helper type 17, Th17) (Higgs, Higgins et al. 2012, Ross, Sutton et al. 2013). Complementary studies have shown that natural infection with *B. pertussis* or immunization with wP vaccines, which contain killed bacteria, promote naïve T-cell differentiation into Th1 and Th17 types, which promote bacterial killing by activation of macrophages and neutrophils and induction of IgG2a opsonizing antibodies. On the contrast, current aP vaccines, containing three to five purified antigens, promote naïve T-cell differentiation into Th17 cells, which activate neutrophils, and Th2 cells, which promote eosinophil activation, with no known protective role, and induction of toxin-

neutralizing IgG1 antibodies (Higgs, Higgins et al. 2012). These findings were also confirmed by a recent study with a baboon model, in which animals showed the same type of immunity response (Warfel, Zimmerman et al. 2014). Importantly, baboons immunized with aP vaccines were protected from pertussis-associated symptoms but not from colonization and were able to transmit the disease to unimmunized animals. By contrast, immunization with wP vaccines resulted in a more rapid *B. pertussis* clearance.

The observation that aP vaccines, which induce a different immune response from natural infection, fail to prevent colonization and transmission, in addition to waning immunity and the emergence of strains with mutated antigens, provides a plausible explanation of pertussis resurgence and suggests that control of the disease requires the development of improved vaccines (Clark, Messonnier et al. 2012).

1.2. Outer Membrane Vesicles

Outer Membrane Vesicles (OMV) are blebs of the outer membrane that are spontaneously released by virtually any Gram-negative bacteria (Haurat, Elhenawy et al. 2015, Schwechheimer and Kuehn 2015). Although the observation of OMV release was made over 40 years ago, only in the past 10 years their study has become focused on their functions and biologica roles, especially as they relate to bacterial pathogenesis. This phenomenon happens in very different settings, including planktonic cultures, surface-attached biofilm communities, solid and liquid media, and natural environments such as fresh and salt water or mammalian hosts (Beveridge, Makin et al. 1997, Beveridge 1999, Hellman, Loiselle et al. 2000, Biller, Schubotz et al. 2014). OMV are spherical and bilyered structure and they range from 50 to 250 nm in size. Clearly, being liberated from the outer membrane, OMV contain lipopolysaccharide (LPS), outer membrane proteins and phospholipids, along with periplasmic proteins in their lumen (McBroom, Johnson et al. 2006).

To better understand the mechanisms that are involved in OMV biogenesis it is important to consider the peculiar architecture of the bacterial cell envelope. Indeed, the budding and detachment of OMV depends on speficic interactions between the bacterial outer membrane and the underlying peptidoglycan layer (Braun and Wolff 1975, Cascales, Bernadac et al. 2002). In particular, specific crosslinks determine envelope stability, give bacteria their shape and confer protection from osmotic changes and sheer stress. OMV biogenesis therefore must rely on the dissociation of the outer membrane from the peptidoglycan layer in specific areas were attachments are depleted or missing. The budding vesicles then bulge outwards until the membrane undergoes fission and detaches (Schwechheimer and Kuehn 2015).

OMV are largely described in literature for their multifaceted roles in bacterial physiology and pathogenesis. The various functions attributed to OMV can be classified in two main groups: response to physical and chemical stress and delivery of biomolecules. Therefore, bacteria can utilize OMV either to improve their chances for survival or to induce changes in their environment, including both the host and the surrounding bacterial community.

Within the first group of biological roles we can list resistance to antibiotics and antimicrobial peptides and protection from antibodies and bacteriophages (Manning and Kuehn 2011). Also, OMV can act to remove toxic compounds from bacterial cells, such as misfolded proteins during temperature stress (McBroom and Kuehn 2007).

On the other hand, within the second group of described functions, we can list different types of OMV cargo, ranging from proteins to saccharides and nucleic acids. OMV are described to stimulate the immune system by presenting antigenic outer membrane components and LPS (Alaniz, Deatherage et al. 2007), to deliver autolysins to competing bacterial species, and to be involved in horizontal DNA transfer (Dorward, Garon et al. 1989). OMV can serve as sources of carbon and nitrogen (Biller, Schubotz et al. 2014), and can carry enzymes able to digest complex biomolecules during nutrient stress (Toledo, Coleman et al. 2012). They were also involved in iron and zinc acquisition, providing bacteria with access to essential metals (Dashper, Hendtlass et al. 2000, Smalley, Byrne et al. 2011, Prados-Rosales, Weinrick et al. 2014). Finally, they were shown to assist in quorum sensing and biofilm formation (Mashburn-Warren, Howe et al. 2009). Most interestingly, when they are released from Gram-negative pathogens, OMV have been found to be enriched with active toxins and other virulence factors that enables them to interact with host cell and contribute to intoxication (Fiocca, Necchi et al. 1999, Kesty, Mason et al. 2004, Chatterjee and Chaudhuri 2011).

2. Chapter one: OMV-based and proteomic driven antigen selection for a new generation vaccine against pertussis

Despite high vaccination coverage world-wide, whooping cough is recently increasing in occurrence suggesting that novel vaccine formulations targeted at the prevention of colonization and transmission should be investigated. In order to identify new candidates for inclusion in the acellular formulation, we used spontaneously released outer membrane vesicles (OMV) as a potential source of key adhesins. The ability of anti-OMV serum to inhibit the adhesion of *B. pertussis* to lung epithelial cells *in vitro* was demonstrated. We employed a proteomic approach to quantify proteins in OMV purified from bacteria in the Bvg+ and Bvg- phase, thus comparing the outer membrane protein pattern of this pathogen in its virulent or avirulent state. Six of the most abundant outer membrane proteins were selected as candidates to be evaluated for their adhesive properties and vaccine potential. We generated *E. coli* strains singularly expressing the selected proteins and assessed their ability to adhere to lung epithelial cells *in vitro*. Four out of the selected proteins conferred adhesive ability to *E. coli*. Three of the candidates were specifically detected by anti-OMV mouse serum suggesting that these proteins are immunogenic antigens able to elicit an antibody response when displayed on the OMV. Anti-OMV serum was able to inhibit only BrkA-expressing *E. coli* adhesion to lung epithelial cells. Finally, stand-alone immunization of mice with recombinant BrkA resulted in significant protection against infection of the lower respiratory tract after challenge with *B. pertussis*. Taken together, these data support the inclusion of BrkA and possibly further adhesins to the current acellular pertussis vaccines to improve the impact of vaccination on the bacterial clearance.

2.1. Results

OMV purification, visualization, enumeration and sizing

In order to identify possible Bvg-regulated outer membrane adhesins, we compared the protein composition of OMV from two *B. pertussis* strains, the Tohama I-derivatives BP536 and BP537 representative of the Bvg+ and Bvg- phases, respectively.

OMV were purified using a detergent-free method from cell-free culture supernatants through ultracentrifugation. Equal amounts with respect to total protein quantities from both preparations were loaded onto SDS-PAGE gel (Fig. 2A) showing significant differences between the two samples representing Bvg+ and Bvg- phases. Several high molecular weight protein bands appear to be exclusive to Bvg+ OMV, as well as two major bands with apparent molecular weight of 42 and 32 kDa, while one intense protein band of apparent molecular weight around 40 kDa seems to be majorly expressed in Bvg- OMV. The 40 kDa protein band was excised, destained and digested with trypsin for peptide mass fingerprinting (PMF) identification: outer membrane porin protein BP0840 was identified with a sequence coverage of 42% (data not shown).

To evaluate the actual number and the size of vesicles we used nanoparticle tracking analysis (NTA), a method for direct, real-time visualization of nanoparticles in liquids through the tracking of the brownian movement of individual particles (Olaya-Abril, Prados-Rosales et al. 2014). OMV samples from BP536 and BP537, normalized to the same protein concentration of 1 mg/mL, contained 6 $x10^{11}$/mL and 6.3 x 10^{11}/mL OMV-particles, respectively. The size distribution of OMV isolated from both strains was in the 70–230 nm diameter range with the majority of the OMV particles at 115 nm (Fig. 2B). These results indicated that, despite the dramatic difference in protein

composition of the two OMV samples, 1 mg of proteins from each OMV preparation as measured with the Lowry assay, corresponds to the same number of vesicles (around 6 x 10^{11} blebs).

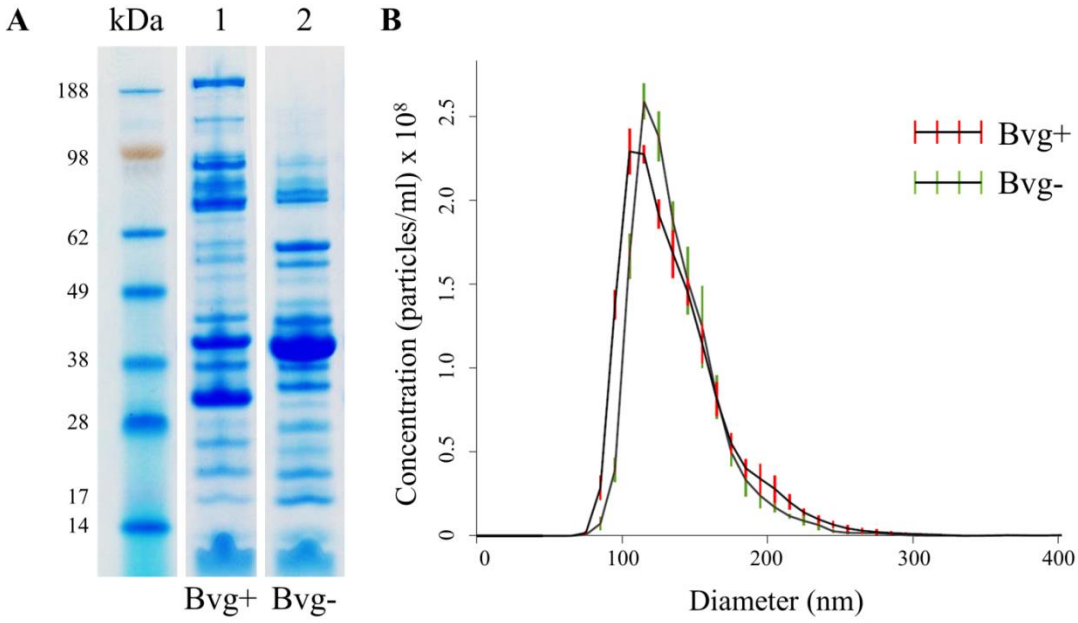

FIG. 2. SDS-PAGE and nanoparticle tracking analysis of OMV samples from BP536 and BP537. (A) SDS-PAGE and Coomassie blue staining of 10 µg (protein content) of OMV samples from *B. pertussis* BP536 Bvg+ (lane 1) and its Bvg- derivative BP537 (lane 2). (B) Nanoparticle tracking analysis measurement of OMV preparation (1 mg protein/mL) showing the sizes and total number of OMV per mL.

Inhibition of *B. pertussis* adhesion with anti-OMV serum

We checked whether antibodies raised against antigens present in Bvg+ OMV could have anti-adhesive properties on *B. pertussis*. We tested the ability of anti-OMV sera to inhibit adhesion of BP536 to A549 respiratory epithelial cells. Fluorescent bacteria were pre-incubated with mouse pooled sera in a range of four dilutions and A549 cells were infected as described previously (Zanaboni, Arato et al. 2016). Mouse anti-sera were raised to Bvg+ OMV and whole bacteria adsorbed to aluminum hydroxide and collected after the third immunization together with control sera from mice immunized with adjuvant only. We found that anti-OMV serum conferred a substantial reduction of adhering bacteria even at low serum concentrations. Interestingly, sera raised against whole bacteria, therefore targeting the entire membrane antigen repertoire, showed a comparable kinetic of inhibition. Anti-alum serum was included in the experiments as negative control and, as expected, did not induce any inhibition of *B. pertussis* adhesion (Fig. 3).

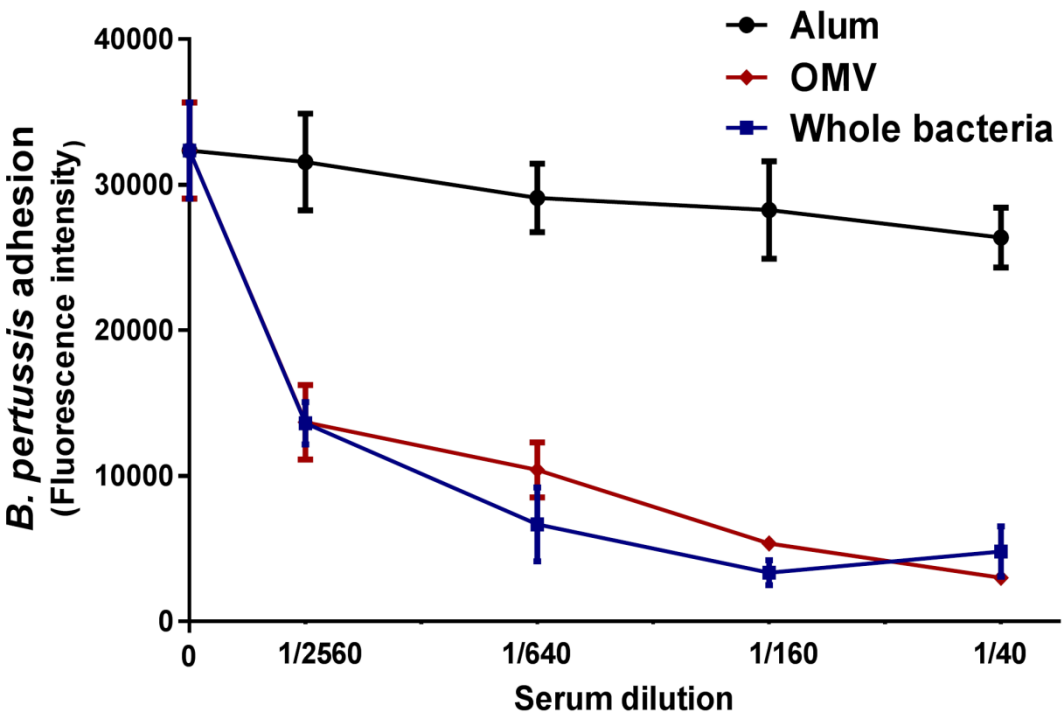

FIG. 3. Impact of anti-OMV serum on *B. pertussis* adhesion to A549 cells. Sera from 10 mice immunized with either OMV, whole bacteria or aluminum hydroxide as control were pooled, serially diluted in infection medium and incubated with labeled wild-type *B. pertussis* BP536 for 1 h. A549 cells were then infected with the bacteria/sera mixtures for 1 hour and, after extensive washes to remove unbound bacteria, cell-associated bacteria were quantified by fluorescence reading at Ex/Em 485/535 nm. Results represent mean ± SD of one representative of three independent experiments each performed in triplicates.

Comparative proteomic analysis

OMV samples from BP536 and BP537 were digested by trypsin after TCA precipitation. Proteomic analysis was performed by LC-MS/MS using a Data-Dependent Acquisition (DDA) approach. A total of 155 and 247 proteins were quantified in the first and second biological replicate respectively, with the second replicate fully including the proteins quantified in the first one. Percentages of each protein in the total samples were averaged to calculate the fold increase of each protein amount in one Bvg phase with the respect to the other (Table 2). Despite some proteins were identified exclusively in either Bvg+ or Bvg- phase, we set a threshold to determine the Bvg phase specificity: 23 proteins showed a 10-fold increase in Bvg+ vs. Bvg- phase and represented ~58% of the total protein amount in Bvg+ OMV while 26 proteins showed a 10-fold increase in Bvg- vs. Bvg+ phase and represented ~14% of the total protein amount in Bvg- OMV (Fig. 4A). The localization of the quantified proteins was predicted according to PSORTb software and refined for lipoprotein annotation using DOLOP software. The analysis predicted ~90% and ~75% of outer membrane proteins, lipoproteins, extracellular and periplasmic proteins for Bvg+ and Bvg- OMV, respectively (Fig. 4B). Around 10% of the identified proteins had an unknown prediction of localization in both OMV samples but only a minority of proteins was predicted to be inner membrane or cytoplasmic, thus confirming that vesicles are generated by outer membrane blebbing and not by bacterial lysis. This analysis confirmed the main differences already observed in the SDS-PAGE gel, identifying the five most abundant proteins in Bvg+ OMV to have a theoretical molecular weight higher than 90 kDa and the most abundant protein in Bvg- OMV to be the outer membrane porin protein BP0840 (~20%).

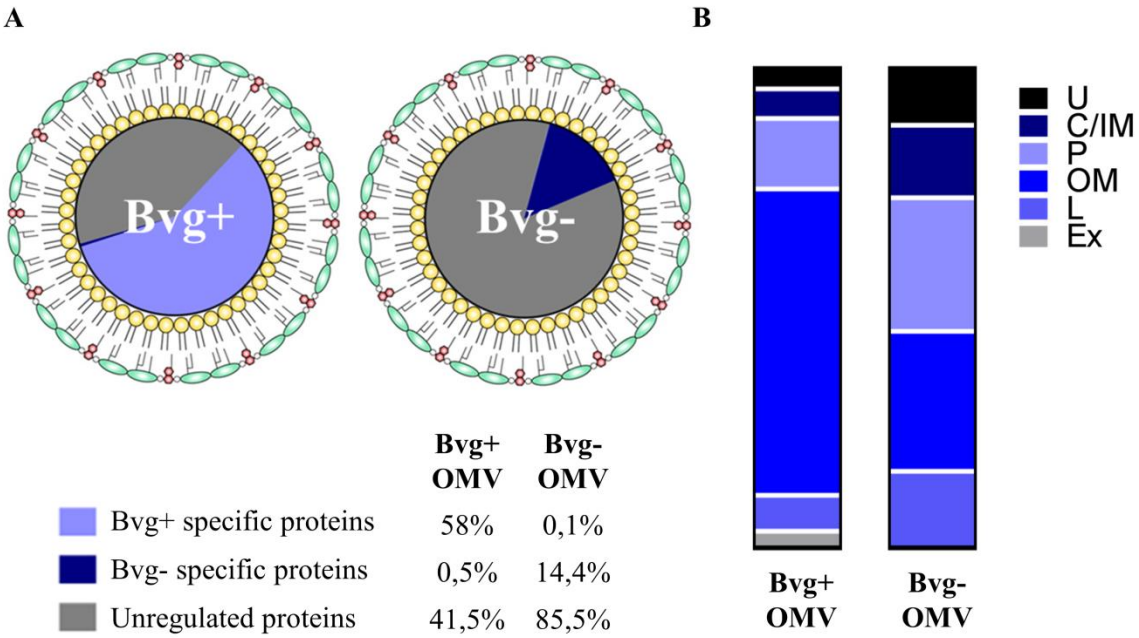

FIG. 4. Comparative proteomic analysis of *B. pertussis* OMV: protein quantification through LC-MS/MS and prediction of their subcellular localization. (A) Protein quantification of Bvg+ and Bvg- OMV: proteins with 10-fold amount increase in Bvg+ vs. Bvg- OMV (light blue), proteins with 10-fold amount increase in Bvg- vs. Bvg+ OMV (dark blue), unregulated proteins (grey). (B) Distribution of quantified proteins in the distinct subcellular localizations based on prediction with PSORTb and DOLOP softwares: Outer Membrane (OM), Periplasm (P), Lipoproteins (L) Inner Membrane (IM), Cytoplasm (C), Extracellular (Ex), Unknown (U).

Accession	Description [Bordetella pertussis Tohama I]	% BVG+	% BVG-	Fold increase Bvg+ vs. Bvg-	Fold increase Bvg- vs. Bvg+	PSORTb	DOLOP
NP_880571.1	filamentous hemagglutinin/adhesin	16,64%	0,01%	1760,96	0,00	Outer Membrane	
NP_882013.1	BrkA autotransporter	11,82%	0,04%	313,79	0,00	Outer Membrane	
NP_879839.1	pertactin autotransporter	8,46%	0,00%	1771,79	0,00	Outer Membrane	
NP_879104.1	autotransporter subtilisin-like protease SphB1	6,50%	0,00%	3284,82	0,00	Outer Membrane	
NP_880953.1	Vag8 autotransporter	4,72%	0,00%	1421,45	0,00	Outer Membrane	
NP_881876.1	translocation protein TolB	3,86%	8,69%	0,44	2,25	Periplasmic	
NP_879974.1	tracheal colonization factor	3,77%	0,00%	3094,18	0,00	Outer Membrane	
NP_879893.1	outer membrane ligand binding protein	3,42%	0,74%	4,60	0,22	Outer Membrane	
NP_879898.1	serotype 2 fimbrial subunit	3,03%	0,00%	5846,89	0,00	Extracellular	
NP_882014.1	molecular chaperone GroEL	2,82%	3,73%	0,75	1,32	Cytoplasmic	
NP_879650.1	outer membrane porin protein BP0840	2,75%	20,28%	0,14	7,38	Outer Membrane	
NP_879093.1	exported protein	2,24%	2,15%	1,04	0,96	Unknown	lipo
NP_882074.1	peptidyl-prolyl cis-trans isomerase	2,19%	2,18%	1,01	0,99	Periplasmic	
NP_882329.1	amino acid ABC transporter substrate-binding protein	1,50%	1,25%	1,20	0,83	Periplasmic	
NP_879666.1	TonB-dependent receptor BfrD	1,48%	0,01%	171,18	0,01	Outer Membrane	
NP_881875.1	peptidoglycan-associated lipoprotein	1,28%	2,76%	0,46	2,15	Outer Membrane	lipo
NP_880337.1	iron binding protein	1,18%	0,37%	3,24	0,31	Periplasmic	
NP_880224.1	ABC transporter substrate-binding protein	1,17%	0,75%	1,56	0,64	Unknown	
NP_881568.1	lipoprotein	1,13%	1,71%	0,66	1,52	Outer Membrane	lipo
NP_879744.1	outer membrane protein A	1,06%	1,26%	0,84	1,19	Outer Membrane	
NP_881062.1	serine protease	0,90%	2,95%	0,31	3,27	Periplasmic	
NP_880436.1	peptidase	0,69%	1,59%	0,43	2,32	Outer Membrane	
NP_881028.1	peptide ABC transporter substrate-binding protein	0,68%	0,01%	58,54	0,02	Periplasmic	
NP_880575.1	filamentous hemagglutinin transporter protein FhaC	0,66%	0,07%	9,06	0,11	Outer Membrane	
NP_879258.1	exported protein	0,61%	1,28%	0,48	2,09	Periplasmic	lipo
NP_880303.1	lipoprotein	0,60%	4,37%	0,14	7,27	Unknown	lipo

NP_879135.1	exported protein	0,56%	0,68%	0,82	1,23	Periplasmic	
NP_880049.1	sn-glycerol-3-phosphate ABC transporter substrate-binding protein UgpB	0,56%	1,82%	0,31	3,27	Periplasmic	
NP_881874.1	hypothetical protein BP3341	0,54%	1,43%	0,38	2,64	Unknown	
NP_879068.1	lipoprotein	0,45%	0,09%	4,83	0,21	Unknown	lipo
NP_881542.1	ABC transporter substrate-binding protein	0,42%	0,33%	1,30	0,77	Unknown	
NP_880721.1	glycine/betaine ABC transporter substrate-binding protein	0,40%	0,61%	0,65	1,53	Periplasmic	
NP_880844.1	outer membrane protein assembly factor BamB	0,37%	0,90%	0,41	2,43	Outer Membrane	
NP_881124.1	zinc protease	0,37%	0,39%	0,94	1,06	Outer Membrane	
NP_879378.1	autotransporter BP0529	0,36%	0,02%	14,91	0,07	Outer Membrane	
NP_881639.1	adenosylhomocysteinase	0,36%	0,18%	2,02	0,49	Cytoplasmic	
NP_881351.1	ABC transporter substrate-binding protein	0,33%	1,64%	0,20	4,97	Periplasmic	
NP_881504.1	TonB-dependent receptor	0,30%	2,76%	0,11	9,33	Outer Membrane	
NP_881019.1	enolase	0,28%	0,39%	0,71	1,40	Cytoplasmic	
NP_880170.1	outer membrane protein	0,27%	0,97%	0,27	3,64	Periplasmic	
NP_881493.1	DNA-binding protein	0,26%	0,03%	9,57	0,10	Unknown	
NP_882283.1	pertussis toxin subunit 2	0,26%	0,00%	#DIV/0!	0,00	Unknown	
NP_879610.1	polyribonucleotide nucleotidyltransferase	0,22%	0,31%	0,72	1,39	Cytoplasmic	
NP_879922.1	outer membrane protein assembly factor	0,22%	0,59%	0,37	2,69	Outer Membrane	lipo
NP_880169.1	outer membrane protein assembly factor	0,22%	0,79%	0,27	3,67	Outer Membrane	
NP_880053.1	leu/Ile/val-binding protein	0,21%	0,46%	0,47	2,13	Periplasmic	
NP_880738.1	efflux system inner membrane protein	0,21%	1,79%	0,12	8,38	Cytoplasmic Membrane	
NP_881866.1	chaperone SurA	0,21%	0,56%	0,38	2,66	Periplasmic	
NP_880063.1	lipoprotein	0,20%	0,61%	0,32	3,10	Unknown	lipo
NP_882317.1	hypothetical protein BP3819	0,19%	0,52%	0,38	2,66	Unknown	
NP_879005.1	penicillin-binding protein	0,19%	1,93%	0,10	10,40	Cytoplasmic Membrane	
NP_879899.1	NADP-dependent malic enzyme	0,18%	0,03%	6,15	0,16	Cytoplasmic	
NP_879406.1	amino acid ABC transporter substrate-binding protein	0,17%	0,83%	0,21	4,80	Periplasmic	

NP_878925.1	elongation factor Tu	0,17%	0,85%	0,20	4,95	Cytoplasmic	
NP_882263.1	lipoprotein	0,15%	0,09%	1,74	0,58	Outer Membrane	lipo
NP_882282.1	pertussis toxin subunit 1	0,15%	0,00%	#DIV/0!	0,00	Extracellular	
NP_879312.1	exported protein	0,15%	7,15%	0,02	47,22	Unknown	
NP_879963.1	lipoprotein	0,15%	0,07%	1,98	0,50	Outer Membrane	lipo
NP_879023.1	glycerol-3-phosphate ABC transporter substrate-binding protein	0,15%	0,00%	145,71	0,01	Periplasmic	
NP_882284.1	pertussis toxin subunit 4	0,14%	0,00%	#DIV/0!	0,00	Unknown	
NP_879606.1	ketol-acid reductoisomerase	0,13%	0,10%	1,33	0,75	Cytoplasmic	
NP_882045.1	DNA-binding protein HU-beta	0,13%	0,07%	1,72	0,58	Unknown	
NP_881135.1	Outer membrane protein assembly factor BamE	0,13%	0,41%	0,31	3,24	Unknown	
NP_880780.1	exported protein	0,12%	0,62%	0,20	4,99	Extracellular	lipo
NP_879256.1	exported protein	0,12%	0,73%	0,17	6,03	Cytoplasmic Membrane	
NP_879501.1	exported protein	0,12%	0,38%	0,32	3,11	Periplasmic	
NP_882347.1	catalase	0,12%	0,08%	1,45	0,69	Periplasmic	
NP_879904.1	2-oxoglutarate dehydrogenase complex subunit dihydrolipoamide succinyltransferase	0,12%	0,05%	2,31	0,43	Cytoplasmic	
NP_882286.1	pertussis toxin subunit 3	0,11%	0,00%	#DIV/0!	0,00	Unknown	
NP_881063.1	sigma factor regulatory protein	0,10%	0,16%	0,62	1,61	Periplasmic	
NP_879065.1	bacterioferritin	0,10%	0,23%	0,42	2,36	Cytoplasmic	
NP_880264.1	extracellular solute-binding protein	0,10%	0,05%	1,90	0,53	Periplasmic	
NP_880329.1	glutamine synthetase	0,10%	0,03%	3,75	0,27	Cytoplasmic	
NP_881814.1	thiol:disulfide interchange protein	0,09%	0,28%	0,33	3,06	Periplasmic	
NP_879452.1	carboxy-terminal processing protease	0,09%	0,27%	0,33	3,05	Cytoplasmic Membrane	
NP_880306.1	glutamine ABC transporter substrate-binding protein	0,08%	0,12%	0,71	1,41	Periplasmic	
NP_881933.1	outer membrane porin protein OmpQ	0,08%	0,00%	#DIV/0!	0,00	Outer Membrane	
NP_881966.1	exported protein	0,08%	0,09%	0,85	1,18	Unknown	
NP_881275.1	ABC transporter substrate-binding protein	0,08%	0,01%	6,87	0,15	Periplasmic	

NP_881784.1	peptide ABC transporter substrate-binding protein	0,08%	0,11%	0,72	1,38	Periplasmic	
NP_880714.2	DNA-binding protein Bph2	0,08%	0,04%	2,14	0,47	Cytoplasmic	
NP_881280.1	adhesin FhaS	0,08%	0,01%	6,30	0,16	Outer Membrane	
NP_880732.1	exported protein	0,07%	0,07%	1,08	0,93	Unknown	
NP_880573.1	outer membrane usher protein FimC	0,07%	0,00%	#DIV/0!	0,00	Outer Membrane	
NP_880572.1	chaperone protein FimB/FhaD	0,07%	0,00%	139,94	0,01	Periplasmic	
NP_879836.1	D-alanyl-D-alanine carboxypeptidase	0,07%	0,91%	0,08	12,67	Periplasmic	
NP_882081.1	exported protein	0,07%	0,02%	3,94	0,25	Periplasmic	
NP_880577.1	exported protein	0,07%	0,08%	0,86	1,17	Periplasmic	
NP_881416.1	lipoprotein	0,07%	0,44%	0,15	6,78	Cytoplasmic Membrane	
NP_882264.1	exported protein	0,06%	0,06%	1,01	0,99	Unknown	
NP_879015.1	thiol:disulfide interchange protein DsbA	0,06%	0,04%	1,77	0,57	Periplasmic	
NP_881828.1	ATP synthase subunit alpha	0,06%	0,01%	4,66	0,21	Cytoplasmic	
NP_881191.1	lipoprotein	0,06%	0,30%	0,20	4,89	Unknown	lipo
NP_881050.1	cytosol aminopeptidase	0,06%	0,04%	1,44	0,70	Cytoplasmic	
NP_881830.1	ATP synthase subunit beta	0,06%	0,01%	6,62	0,15	Cytoplasmic	
NP_879712.1	peptidase	0,06%	0,04%	1,32	0,76	Unknown	
NP_880524.1	glycerol-3-phosphate ABC transporter substrate-binding protein	0,06%	0,05%	1,03	0,97	Periplasmic	
NP_879609.1	30S ribosomal protein S15	0,05%	0,07%	0,80	1,25	Cytoplasmic	
NP_879842.1	membrane protein	0,05%	0,02%	2,78	0,36	Unknown	
NP_880735.1	lipoprotein	0,05%	0,15%	0,36	2,75	Unknown	lipo
NP_880592.1	peptidyl-prolyl cis-trans isomerase B	0,05%	0,12%	0,42	2,39	Cytoplasmic	
NP_882088.1	exported protein	0,05%	0,01%	9,19	0,11	Unknown	
NP_880868.1	autotransporter	0,05%	0,11%	0,46	2,20	Outer Membrane	
NP_881247.1	inosine-5'-monophosphate dehydrogenase	0,05%	0,05%	1,01	0,99	Cytoplasmic	
NP_880725.1	beta-ketothiolase	0,05%	0,07%	0,65	1,54	Cytoplasmic	
NP_881631.1	transglycosylase	0,04%	0,19%	0,23	4,34	Periplasmic	

NP_880879.1	type III secretion protein	0,04%	0,00%	9,48	0,11	Outer Membrane	
NP_879855.1	phosphate ABC transporter substrate-binding protein PstS	0,04%	0,16%	0,27	3,68	Periplasmic	
NP_880574.1	fimbrial adhesin	0,04%	0,00%	#DIV/0!	0,00	Extracellular	
NP_880108.1	exported protein	0,04%	0,02%	2,51	0,40	Unknown	
NP_881812.1	membrane-bound transglycosylase	0,04%	0,19%	0,20	5,02	Unknown	lipo
NP_881126.1	chaperone protein DnaK	0,04%	0,07%	0,52	1,91	Cytoplasmic	
NP_879408.1	exported protein	0,04%	0,05%	0,78	1,29	Periplasmic	
NP_882325.1	exported protein	0,04%	0,06%	0,66	1,52	Unknown	
NP_882066.1	peroxiredoxin	0,04%	0,03%	1,25	0,80	Cytoplasmic	
NP_882235.1	exported protein	0,04%	0,07%	0,49	2,03	Outer Membrane	
NP_879409.1	exported protein	0,04%	0,08%	0,44	2,28	Unknown	
NP_880114.1	amino acid ABC transporter substrate-binding protein	0,03%	1,48%	0,02	44,97	Periplasmic	
NP_879067.1	lipoprotein	0,03%	0,06%	0,51	1,97	Unknown	lipo
NP_880267.1	amino acid-binding periplasmic protein	0,03%	0,01%	3,20	0,31	Periplasmic	
NP_879314.1	heme receptor HemC	0,03%	0,00%	8,17	0,12	Outer Membrane	
NP_879807.1	exported protein	0,03%	0,16%	0,18	5,43	Unknown	lipo
NP_881587.1	membrane protein	0,03%	0,03%	0,97	1,03	Unknown	
NP_881196.1	lipoprotein	0,03%	0,13%	0,21	4,73	Unknown	lipo
NP_879636.1	azurin	0,03%	0,08%	0,34	2,95	Periplasmic	
NP_880994.1	citrate synthase	0,03%	0,07%	0,39	2,58	Cytoplasmic	
NP_880045.1	leucine/isoleucine/valine ABC transporter substrate-binding protein	0,03%	0,02%	1,17	0,86	Periplasmic	
NP_882085.1	glycine/betaine ABC transporter substrate-binding protein	0,03%	0,06%	0,47	2,14	Periplasmic	
NP_881539.1	N-acetyl-gamma-glutamyl-phosphate reductase	0,03%	0,01%	2,18	0,46	Cytoplasmic	
NP_880241.1	amino acid ABC transporter substrate-binding protein	0,03%	0,07%	0,37	2,72	Unknown	
NP_881692.1	outer membrane lipoprotein LolB	0,02%	0,09%	0,29	3,48	Unknown	lipo
NP_882015.1	co-chaperonin GroES	0,02%	0,12%	0,19	5,19	Cytoplasmic	
NP_881501.1	lipoprotein	0,02%	0,08%	0,28	3,63	Outer Membrane	lipo

NP_879524.1	lipoprotein	0,02%	0,06%	0,35	2,85	Unknown	lipo
NP_879539.1	aspartate--tRNA ligase	0,02%	0,02%	1,30	0,77	Cytoplasmic	
NP_881365.1	superoxide dismutase	0,02%	0,03%	0,78	1,28	Periplasmic	
NP_882357.1	peptide ABC transporter substrate-binding protein	0,02%	0,01%	4,17	0,24	Periplasmic	
NP_881413.1	hypothetical protein BP2815	0,02%	0,01%	2,46	0,41	Unknown	
NP_881382.1	lipoprotein	0,02%	0,02%	1,32	0,76	Unknown	lipo
NP_879179.1	ABC transporter substrate-binding protein	0,02%	0,04%	0,52	1,92	Periplasmic	
NP_880217.1	exported protein	0,02%	0,11%	0,19	5,40	Unknown	
NP_882152.1	50S ribosomal protein L17	0,02%	0,04%	0,48	2,08	Cytoplasmic	
NP_879154.1	stringent starvation protein A	0,02%	0,01%	1,38	0,72	Cytoplasmic	
NP_881865.1	LPS-assembly protein LptD	0,02%	0,04%	0,51	1,98	Outer Membrane	
NP_880864.1	cell surface protein	0,02%	0,03%	0,62	1,62	Unknown	
NP_879131.1	N-acetylmuramoyl-L-alanine amidase	0,02%	0,02%	0,81	1,23	Cytoplasmic	
NP_880586.1	exported protein	0,02%	0,02%	0,72	1,39	Unknown	
NP_881648.1	outer membrane protein	0,02%	0,16%	0,11	9,23	Outer Membrane	
NP_879309.1	acetylornithine transaminase	0,02%	0,04%	0,40	2,50	Cytoplasmic	
NP_879334.1	sulfite oxidase subunit YedY	0,02%	0,00%	18,90	0,05	Unknown	
NP_880221.1	aspartate-semialdehyde dehydrogenase	0,02%	0,07%	0,22	4,50	Cytoplasmic	
NP_881167.1	succinyl-CoA ligase subunit alpha	0,02%	0,49%	0,03	31,90	Cytoplasmic	
NP_880986.1	putrescine ABC transporter substrate-binding protein	0,02%	0,02%	0,62	1,61	Periplasmic	
NP_881001.1	malate dehydrogenase	0,02%	0,04%	0,39	2,56	Cytoplasmic	
NP_882247.1	cytochrome c oxidase subunit 2	0,02%	0,04%	0,38	2,65	Cytoplasmic Membrane	
NP_880476.1	2 3 4 5-tetrahydropyridine-2 6-carboxylate N-succinyltransferase	0,01%	0,01%	1,27	0,79	Cytoplasmic	
NP_881473.1	c'cytochrome	0,01%	0,03%	0,55	1,81	Periplasmic	
NP_880458.1	peptidoglycan-binding protein	0,01%	0,02%	0,62	1,62	Cytoplasmic Membrane	
NP_879905.1	2-oxoglutarate dehydrogenase complex subunit dihydrolipoamide dehydrogenase	0,01%	0,01%	2,66	0,38	Cytoplasmic	

NP_880776.1	glutathione reductase	0,01%	0,02%	0,65	1,54	Cytoplasmic	
NP_881115.1	isocitrate dehydrogenase	0,01%	0,09%	0,14	6,94	Cytoplasmic	
NP_882134.1	aldehyde dehydrogenase	0,01%	0,01%	1,66	0,60	Cytoplasmic	
NP_879841.1	membrane protein	0,01%	0,02%	0,58	1,74	Unknown	
NP_881695.1	cyclase	0,01%	0,04%	0,27	3,74	Cytoplasmic	
NP_881693.1	hypothetical protein BP3128	0,01%	0,02%	0,69	1,46	Unknown	
NP_881168.1	succinyl-CoA ligase subunit beta	0,01%	0,13%	0,09	11,44	Cytoplasmic	
NP_881781.1	osmotically inducible lipoprotein B	0,01%	0,03%	0,39	2,60	Unknown	lipo
NP_882271.1	imidazoleglycerol-phosphate dehydratase	0,01%	0,01%	1,29	0,78	Cytoplasmic	
NP_881374.1	short-chain dehydrogenase	0,01%	0,04%	0,30	3,32	Cytoplasmic	
NP_880304.1	4-hydroxy-tetrahydrodipicolinate synthase	0,01%	0,01%	1,07	0,94	Cytoplasmic	
NP_880836.1	adenylosuccinate synthetase	0,01%	0,02%	0,60	1,68	Cytoplasmic	
NP_882170.1	single-strand DNA-binding protein	0,01%	0,02%	0,68	1,48	Cytoplasmic	
NP_881665.1	molybdate ABC transporter substrate-binding protein ModA	0,01%	0,30%	0,03	31,87	Periplasmic	
NP_879417.1	exported protein	0,01%	0,09%	0,10	9,98	Unknown	
NP_879686.1	lipoprotein	0,01%	0,02%	0,45	2,25	Unknown	lipo
NP_880302.1	serotype 3 fimbrial subunit	0,01%	0,00%	8,55	0,12	Extracellular	
NP_879680.1	exported protein	0,01%	0,02%	0,53	1,89	Unknown	
NP_880801.1	exported protein	0,01%	0,00%	15,11	0,07	Unknown	
NP_882120.1	elongation factor G	0,01%	0,07%	0,12	8,10	Cytoplasmic	
NP_880162.1	elongation factor Ts	0,01%	0,03%	0,28	3,60	Cytoplasmic	
NP_882233.1	bifunctional UDP-N-acetylglucosamine pyrophosphorylase/glucosamine-1-phosphate N-acetyltransferase	0,01%	0,01%	0,81	1,23	Cytoplasmic	
NP_879756.1	ADP-L-glycero-D-manno-heptose-6-epimerase	0,01%	0,01%	0,88	1,13	Cytoplasmic	
NP_879343.1	DNA polymerase III subunit beta	0,01%	0,01%	0,73	1,36	Cytoplasmic	
NP_880296.1	exported protein BP1561	0,01%	0,00%	6,29	0,16	Outer Membrane	
NP_878933.1	DNA-directed RNA polymerase subunit beta'	0,01%	0,03%	0,27	3,65	Cytoplasmic	
NP_881287.1	fimbrial protein	0,01%	0,00%	63,65	0,02	Extracellular	

NP_881651.1	ABC transporter substrate-binding protein	0,01%	0,02%	0,42	2,37	Cytoplasmic Membrane	
NP_879451.1	peptidase	0,01%	0,06%	0,12	8,40	Unknown	
NP_879765.1	antioxidant protein	0,01%	0,55%	0,01	78,08	Cytoplasmic	
NP_881266.1	exported protein	0,01%	0,02%	0,44	2,29	Unknown	
NP_879209.1	exported protein	0,01%	0,01%	0,64	1,56	Periplasmic	
NP_880834.1	30S ribosomal protein S21	0,01%	0,01%	0,61	1,63	Cytoplasmic	
NP_880684.1	aconitate hydratase	0,01%	0,11%	0,06	16,49	Cytoplasmic	
NP_881490.1	phospho-2-dehydro-3-deoxyheptonate aldolase	0,01%	0,03%	0,21	4,69	Cytoplasmic	
NP_878936.1	peptidoglycan-binding protein	0,01%	0,02%	0,40	2,53	Unknown	
NP_881498.1	nucleotide-binding protein	0,01%	0,01%	0,78	1,28	Cytoplasmic	
NP_879794.1	glyceraldehyde-3-phosphate dehydrogenase	0,01%	0,99%	0,01	163,89	Cytoplasmic	
NP_879530.1	exported protein	0,01%	0,01%	0,52	1,92	Unknown	
NP_880485.1	trigger factor	0,01%	0,01%	0,55	1,83	Cytoplasmic	
NP_880438.1	exported protein	0,01%	0,07%	0,08	11,99	Periplasmic	
NP_882258.1	outer membrane protein	0,01%	0,01%	0,76	1,31	Outer Membrane	
NP_880997.1	succinate dehydrogenase flavoprotein subunit	0,01%	0,02%	0,25	3,94	Cytoplasmic Membrane	
NP_881474.1	adenylosuccinate lyase	0,01%	0,00%	1,88	0,53	Cytoplasmic	
NP_879519.1	exported protein	0,01%	0,01%	0,62	1,61	Periplasmic	
NP_880710.1	LPS-assembly lipoprotein LptE	0,00%	0,02%	0,22	4,61	Unknown	lipo
NP_879616.1	triosephosphate isomerase	0,00%	0,00%	0,97	1,03	Cytoplasmic	
NP_882148.1	30S ribosomal protein S13	0,00%	0,01%	0,68	1,47	Cytoplasmic	
NP_882131.1	50S ribosomal protein L29	0,00%	0,00%	1,54	0,65	Cytoplasmic	
NP_881531.1	serine hydroxymethyltransferase	0,00%	0,04%	0,10	9,79	Cytoplasmic	
NP_882109.1	thiazole synthase	0,00%	0,00%	0,96	1,04	Cytoplasmic	
NP_880202.1	lipoprotein	0,00%	0,01%	0,23	4,33	Unknown	lipo
NP_882053.1	ornithine carbamoyltransferase	0,00%	0,01%	0,32	3,11	Cytoplasmic	
NP_881859.1	binding-protein-dependent transport protein	0,00%	0,02%	0,21	4,74	Periplasmic	

NP_881497.1	exported protein	0,00%	0,01%	0,30	3,36	Periplasmic	
NP_880599.1	aspartate kinase	0,00%	0,03%	0,12	8,20	Cytoplasmic	
NP_881402.1	exported protein	0,00%	0,02%	0,20	4,98	Unknown	
NP_881354.1	lipoprotein	0,00%	0,05%	0,06	15,65	Unknown	lipo
NP_882097.1	hypothetical protein BP3584	0,00%	0,01%	0,34	2,96	Cytoplasmic	
NP_880178.1	phosphoenolpyruvate synthase	0,00%	0,02%	0,15	6,82	Cytoplasmic	
NP_882020.1	exported protein	0,00%	0,02%	0,16	6,34	Periplasmic	
NP_879943.1	muramoyltetrapeptide carboxypeptidase	0,00%	0,01%	0,18	5,48	Unknown	
NP_881202.1	50S ribosomal protein L20	0,00%	0,00%	0,54	1,84	Cytoplasmic	
NP_881446.1	aromatic amino acid aminotransferase	0,00%	0,02%	0,15	6,81	Cytoplasmic	
NP_879766.1	sulfate-binding protein	0,00%	0,06%	0,04	25,87	Periplasmic	
NP_879832.1	secreted protein	0,00%	0,00%	0,86	1,17	Cytoplasmic Membrane	
NP_880073.1	bacterioferritin comigratory protein	0,00%	0,00%	0,51	1,96	Unknown	
NP_879384.1	carboxymuconolactone decarboxylase	0,00%	0,00%	137,64	0,01	Unknown	
NP_880450.1	exported protein	0,00%	0,01%	0,18	5,51	Periplasmic	
NP_881385.1	aminotransferase	0,00%	0,01%	0,20	5,12	Cytoplasmic	
NP_881159.1	hypothetical protein BP2532	0,00%	0,01%	0,20	5,07	Cytoplasmic	
NP_880356.1	capsular polysaccharide export protein	0,00%	0,04%	0,04	24,39	Outer Membrane	lipo
NP_880501.1	aromatic amino acid aminotransferase	0,00%	0,02%	0,11	9,33	Cytoplasmic	
NP_880234.1	translation initiation factor IF-3	0,00%	0,01%	0,19	5,14	Cytoplasmic	
NP_879751.2	30S ribosomal protein S1	0,00%	0,02%	0,09	11,40	Cytoplasmic	
NP_879762.1	electron transfer flavoprotein subunit beta	0,00%	0,02%	0,07	13,64	Cytoplasmic	
NP_879972.1	chaperone protein ClpB	0,00%	0,02%	0,07	14,45	Cytoplasmic	
NP_882128.1	50S ribosomal protein L22	0,00%	0,00%	0,30	3,29	Cytoplasmic	
NP_881779.1	cell division topological specificity factor	0,00%	0,00%	0,20	5,07	Cytoplasmic	
NP_879190.1	glutamate-1-semialdehyde 2 1-aminomutase	0,00%	0,01%	0,05	19,12	Cytoplasmic	
NP_879798.1	phosphate acetyltransferase	0,00%	0,01%	0,05	20,77	Unknown	

NP_882151.1	DNA-directed RNA polymerase subunit alpha	0,00%	0,01%	0,05	20,29	Cytoplasmic
NP_881778.1	septum site-determining protein	0,00%	0,01%	0,02	41,37	Cytoplasmic
NP_882254.1	alcohol dehydrogenase	0,00%	0,01%	0,00	204,68	Cytoplasmic
NP_881994.1	phosphopantetheine adenylyltransferase	0,00%	0,01%	0,00	417,36	Cytoplasmic
NP_880652.1	succinate-semialdehyde dehydrogenase	0,00%	0,02%	0,00	#DIV/0!	Cytoplasmic
NP_879763.1	electron transfer flavoprotein subunit alpha	0,00%	0,06%	0,00	#DIV/0!	Unknown
NP_881967.1	hypothetical protein BP3441	0,00%	0,01%	0,00	#DIV/0!	Unknown

Table 2. Comparative proteomics data: proteins quantified in OMV from BP536 and BP537. With LC-MS-MS analysis, 247 proteins were identified and quantified in two biological replicates of Bvg+ (BP536) and Bvg- (BP537) OMV. For each protein, accession number and protein description of *B. pertussis* Tohama I database are listed. In addition, the average (n=2 biological replicates, n=3 technical replicates) of the calculated percentage for each protein in the total sample is given (Average area*MolecularWeight/Sum(Average area*MolecularWeight)). Finally, the fold increase of each protein amount in Bvg+ vs. Bvg- and Bvg- vs. Bvg+ is reported together with the PSORTb and DOLOP prediction of subcellular localization.

Vaccine antigen selection

We applied two main criteria for antigen selection: putative antigens should be either Bvg+ exclusive or showing at least a 2.5 fold increase as compared to Bvg- and they should have a predicted outer membrane localization according to PSORTb. The list of the resulting selected antigens is reported in Table 3. Based on their high abundance in OMV (each higher than 1% of total protein amount) and excluding the proteins already part of the currently available aP formulation, we focused on six promising candidates to be assessed for their adhesive properties and vaccine potential: BrkA, Vag8, TcfA, SphB1, BipA and BfrD. Interestingly, five of the selected antigens had a predicted autotransporter structure.

Accession	Protein name	% Bvg+	% Bvg-
NP_880571.1	FHA filamentous hemagglutinin/adhesin §#	16,64%	0,01%
NP_882013.1	BrkA autotransporter* #	11,82%	0,04%
NP_879839.1	Prn Pertactin autotransporter §#	8,46%	0,00%
NP_879104.1	SphB1 autotransporter subtilisin-like protease* #	6,50%	0,00%
NP_880953.1	Vag8 autotransporter* #	4,72%	0,00%
NP_879974.1	TcfA tracheal colonization factor* #	3,77%	0,00%
NP_879893.1	BipA outer membrane ligand binding protein* #	3,42%	0,74%
NP_879666.1	BfrD TonB-dependent receptor*	1,48%	0,01%
NP_880575.1	FhaC filamentous hemagglutinin transporter protein	0,66%	0,07%
NP_879378.1	BP0529 autotransporter	0,36%	0,02%
NP_881933.1	OmpQ outer membrane porin protein	0,08%	0,00%
NP_881280.1	Adhesin FhaS	0,08%	0,01%
NP_880573.1	FimC outer membrane usher protein	0,07%	0,00%
NP_880879.1	Type III secretion protein	0,04%	0,00%
NP_879314.1	Heme receptor HemC	0,03%	0,00%
NP_880296.1	Exported protein BP1561	0,01%	0,00%

Table 3. OMV-based antigen selection. Antigens were selected from the total proteins quantified in OMV based on the following criteria**:** Bvg regulation, localization prediction and abundance. Percentages refer to the total protein composition of OMV from either Bvg+ or Bvg- phase averaged between the two biological replicates. # known *B. pertussis* protective antigens *=antigen selected for further analysis, §=antigen currently included in a commercial vaccine.

Recombinant *E. coli* strains adhesion and adhesion inhibition assays

In order to evaluate the adhesive properties of each single protein we exploited *E. coli* as an heterologous background system for surface exposure of the selected antigens. We generated *E. coli* strains constitutively expressing the selected full length proteins and checked for their ability to bind to A549 respiratory epithelial cells as compared to wild type *E. coli*. A549 cells were infected with *E. coli* strains for three hours, then washed to remove unbound bacteria, fixed and stained with an anti-*E. coli* antibody. We found that BrkA, SphB1, Vag8 and TcfA conferred adhesive ability to *E. coli* when expressed on the membrane. On the contrary, heterologous expression of BipA and BfrD had no effect on strain adhesiveness (Fig. 5A). We continued the analysis by testing if the *E. coli* strains singularly expressing the selected antigens were detected with the anti-OMV serum we had generated. By flow cytometry, anti-OMV serum was able to recognize the specific heterologously expressed BrkA, Vag8 and BipA (Fig. 5B). This result proved not only that BrkA, Vag8 and BipA antibodies had been elicited after mice immunization with *B. pertussis* OMV but also that these proteins are properly expressed and surface-exposed on *E. coli*. Finally, to determine whether the inhibition of *B. pertussis* adhesion promoted by anti-OMV serum correlated with the presence of specific antibodies against the selected antigens we tested its inhibitory effect on the adhesion of recombinant *E. coli* strains. We found that anti-OMV serum caused reduction of adhering *E. coli* at high serum concentration only when BrkA was expressed on the bacterial surface. Unexpectedly, Vag8-expressing *E. coli* was not inhibited despite the presence of specific anti-Vag8 antibodies in the serum (Fig. 5C).

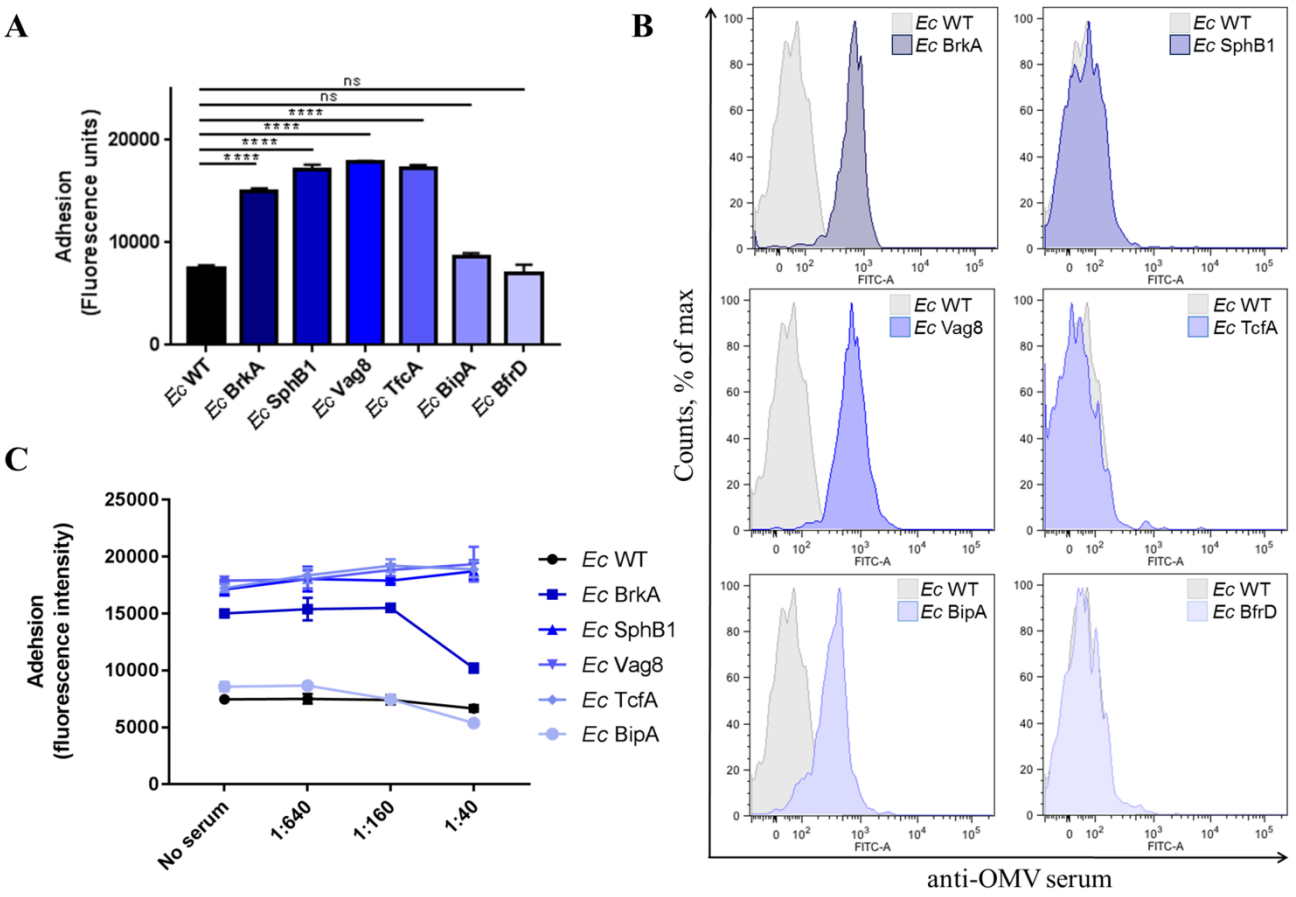

FIG. 5. Functional and immunological characterization of the selected antigens heterologously expressed on *E. coli*. A. Adhesion of recombinant *E. coli* strains on A549 cells. A549 cells were infected with bacteria for 3 hours. Cell-associated bacteria were quantified by fluorescence reading after staining with a rabbit anti-*E. coli* antibody. Results represent mean ± SD of one representative of three independent experiments each performed in triplicates, ****=$P < 0.0001$, ns= non-significant. **B.** FACS analysis on recombinant *E. coli* strain with anti-OMV serum: recombinant *E. coli* strains were collected in early exponential phase, stained with mouse anti-OMV antibody and finally fixed with 3.7% formaldehyde. Recognition of surface exposed *B. pertussis* antigens was checked by flow cytometry using FACS Canto II flow cytometer (BD Biosciences). **C.** Impact of anti-OMV serum on *E. coli* adhesion to A549 cells: anti-OMV serum was serially diluted in infection medium and incubated with recombinant *E. coli* strains for 1 h. A549 cells were then infected with the bacteria/sera mixtures for 3 hours and cell-associated bacteria were quantified by fluorescence reading. Results represent mean ± SD of one representative of three independent experiments each performed in triplicates.

Recombinant BrkA protein production and vaccination

To analyze the protective potential of BrkA, recombinant His-tagged protein was expressed, purified and used to immunize mice three times, four weeks apart. Fifteen days after the final vaccination, mice were challenged with aerosolized *B. pertussis* and seven days later the bacterial load in the lungs was evaluated by CFU counting. This experiment showed that immunization with recombinant BrkA resulted in about 100 fold reduction of bacterial load in the lung as compared to control mice treated with adjuvant only (Fig. 6).

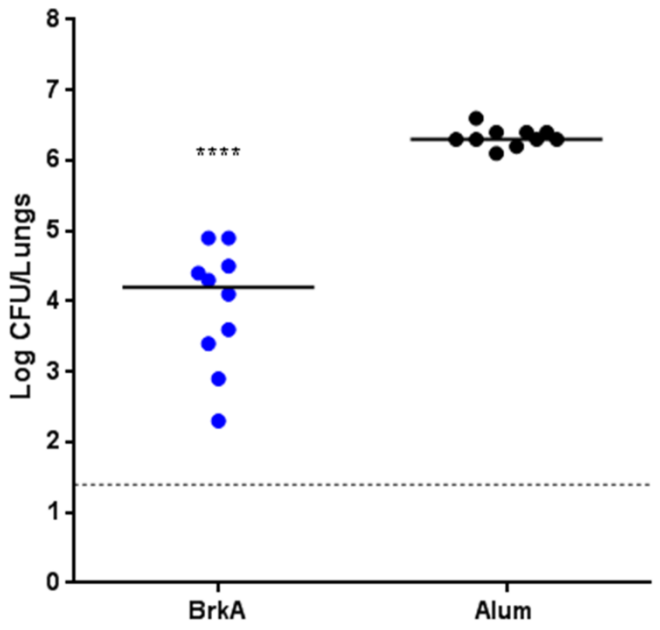

FIG. 6. Protection induced by BrkA in the mouse *B. pertussis* aerosol challenge model: *B. pertussis* infection was followed by performing CFU counts on lungs from groups of 10 mice seven days after aerosol challenge. Protection is reported as compared to mice immunized with the adjuvant only. Results represent mean ± SD; ****=$P < 0.0001$.

2.2 Discussion and conclusions

The increase in pertussis outbreaks and the recent observations with the employment of the baboon model for pertussis infection clearly indicated that a more potent vaccine is needed to prevent not only the disease but also the colonization and therefore transmission of the bacterium. The control of the bacterial burden is governed by multiple mechanisms leading to bacterial killing and interference to the infection process. Among them, the presence of functional antibodies at the epithelial barrier able to target key adhesins is a valuable countermeasure to inhibit the attachment of bacteria and initiation of colonization. In this study, we used outer membrane vesicles to identify potential novel antigens with adhesive properties. Indeed, OMV mainly contain outer membrane proteins and lipoproteins in the membrane bilayer and periplasmic proteins in their lumen. Aiming at preventing *B. pertussis* colonization of the human respiratory tract, we checked the ability of anti-OMV serum to inhibit *B. pertussis* adhesion on A549 respiratory epithelial cells. Interestingly, anti-OMV serum proved to be particularly powerful in preventing *B. pertussis* adhesion to respiratory epithelial cells. Clearly, the whole inhibitory effect on bacterial adhesion is likely determined by the additive effects of different antibodies targeting various antigens displayed by OMV and present on *B. pertussis* surface. We therefore decided to deepen the analysis at the single protein level, looking for proteins present in OMV that could elicit anti-adhesive antibodies after immunization. The comparative proteomic analysis between OMV from Bvg+ and Bvg- allowed the identification and quantification of over two hundred proteins and showed that ~58% of proteins quantified in Bvg+ OMV are specific for that phase and their amount drops to ~0,1% in Bvg- OMV. This finding is in agreement with the well-established regulation of the virulence genes by the BvgAS two-component system in *B. pertussis*. Interestingly, among the 23 Bvg+ specific proteins,

10 proteins were predicted to be outer membrane proteins and represented ~53% of the total Bvg+ OMV protein amount. Among the Bvg+ specific proteins we found the best known and characterized *B. pertussis* adhesins such as FHA, 69K and Fimbriae together with Pertussis Toxin. On the contrary, Adenylate Cyclase Toxin and Dermonecrotic Toxin were not identified. On the other hand, the majority of Bvg- specific proteins appeared to be cytoplasmic contaminants, possibly indicating that *B. pertussis* strain BP537 is more prone to lyse during growth. Finally, among the proteins that did not result to be specific for one or the other phase, the analysis showed a slightly increased amount of lipoproteins, outer membrane and periplasmic proteins in Bvg- OMV vs. Bvg+ OMV. Therefore, it is tempting to hypothesize that most of the proteins in Bvg- OMV are overrepresented to compensate for the lack of the Bvg+ outer membrane proteins and the outer membrane porin protein BP0840 perfectly supported this hypothesis, resulting to be the most abundant protein in Bvg- OMV and representing ~20% of the total protein amount as compared to ~2.5% in Bvg+ OMV. The NTA analysis further supported the hypothesis of a compensative mechanism, showing no differences in size distribution and quantity of proteins per vesicle in both OMV samples. The protein composition of OMV described in the present study differs substantially from what has been shown in a previous report (Raeven, van der Maas et al. 2015). While the high quantity of BrkA and Vag8 is confirmed in both studies, the overall composition in terms of presence and relative abundance is drastically different. This is likely due to the distinct OMV purification methods and *B. pertussis* strains employed in the two studies. The proteomic analysis presented in this study allowed the identification of an initial list of putative antigens, which were narrowed down to 16 interesting candidates: this first antigen selection resulted in seven known *B. pertussis* protective antigens including two of the current aP antigens, thus validating our strategy to identify virulence factors. It is intriguing to underline that proteomic analysis of two

currently circulating *B. pertussis* strains under *in vitro* Bvg+ and Bvg- conditions (de Gouw, de Jonge et al. 2014), combined to *in silico* prediction for surface- expression, resulted in a panel of top 15 candidates which perfectly mirrors the OMV-based antigen selection described in our study. Then, albeit with variations in the strains and methods employed, the membrane composition of OMV seems to closely reflect the composition of whole bacteria. We decided to focus our attention on the most abundant Bvg+ outer membrane proteins and interestingly five autotransporter proteins were at the top of our list. Autotransporters are possibly the simplest bacterial secretion systems (type V): they consist only of a single polypeptide chain organized in a passenger and translocator domain and they have the ability to autonomously translocate across the outer membrane (Fan, Chauhan et al. 2016). Therefore, the heterologous expression of the autotransporters on the surface of *E. coli* was selected to characterize their adhesive properties. This approach allowed the demonstration that BrkA, TcfA, SphB1 and Vag8 conferred to *E. coli* a significant increased ability to adhere to lung epithelial cells. To the best of our knowledge, this is the first time that *B. pertussis* autotransporters were rationally characterized for their adhesive properties exploiting a heterologous *E. coli* background. The involvement in adhesion of BrkA was previously demonstrated in *in vitro* analysis and in mouse infection studies with *B. pertussis* mutant strains showing 2-fold and 2-log reduction in the ability to adhere to cell lines and to colonize the murine lungs, respectively (Fernandez and Weiss 1994, Elder and Harvill 2004). Also, the loss of TcfA was previously shown to cause 10-fold reduction in the number of bacteria isolated from tracheas after *B. pertussis* aerosol challenge (Finn and Stevens 1995). Nevertheless, deletion of individual virulence factor genes could have limited effects on the ability of *B. pertussis* to efficiently infect the respiratory tract of mice, suggesting they may perform redundant functions. This was the case of a Vag8 deletion mutant, which was as efficient as the parental *B. pertussis* strain in colonizing murine lungs

(Finn and Amsbaugh 1998). On the contrary, our study proved that Vag8 is also involved in adhesion and not only in serum resistance as previously described (Marr, Shah et al. 2011). In other cases, the generation of single knock-outs could be misleading. In fact, SphB1 loss has an indirect effect on Filamentous Hemagglutinin which is not cleaved anymore from *B. pertussis* surface therefore rendering the mutant strain even more adhesive than the wild-type parental strain (Coutte, Alonso et al. 2003) but in this study we showed that SphB1 itself can contribute to the overall adhesiveness of *B. pertussis*. Two of the heterogously expressed antigens, BipA and BfrD, did not confer an adhesive phenotype to *E. coli*. While this result could be expected for BfrD, which is reported to be involved in iron acquisition (Brickman, Suhadolc et al. 2015), it was quite controversial for BipA, which is partially characterized in the literature as the major adhesin in the intermediate phase between Bvg+ and Bvg- (Stockbauer, Fuchslocher et al. 2001). This particular virulence phase (Bvg^i) was described to be involved in the transmission of *B. pertussis* from host to host and a BipA deletion mutant of a Bvg^i-locked *B. pertussis* strain displayed a reduced ability to colonize the nasal cavity of mice compared with the parental strain (Vergara-Irigaray, Chavarri-Martinez et al. 2005). BipA was also identified as the most abundant surface-associated biofilm protein (de Gouw, Serra et al. 2014) therefore it is likely involved in bacterium-bacterium interactions as well as host-pathogen interactions. Our results were in contrast with the previous reports but, in the absence of specific antibodies, we could not rule out that BipA is not properly expressed and surface exposed on *E. coli*. We therefore took advantage of sera raised against OMV to explore whether the heterologously expressed antigens were recognized on the surface of *E. coli*. Only three proteins, BrkA, Vag8 and BipA, were specifically recognized on *E. coli* surface by anti-OMV serum, thus excluding the possibility that BipA was not properly surface-exposed on the outer membrane. Finally, we checked the ability of anti-OMV serum to inhibit

recombinant *E. coli* adhesion to lung A549 cells. The inhibitory effect of anti-OMV serum was only observed on the adhesion of BrkA-expressing *E. coli*, demonstrating the functionality of anti-BrkA antibodies. Consistently with the fact that SphB1 and TcfA-expressing *E. coli* strains were not recognized by anti-OMV serum, no inhibition was observed on the adhesiveness of these strains. On the contrary, anti-OMV serum was not able to inhibit Vag8-expressing *E. coli* strain; whether this is due to low antibodies level or to weak antibody functionality needs further clarification. As far as BfrD is concerned, it did not result to have a contribution in adhesion nor to be recognized by anti-OMV serum on *E. coli* surface, therefore was excluded from the adhesion inhibition assay. Still, given its predicted structure of integral outer membrane protein, we cannot exclude that it is not properly expressed on the surface of *E. coli*. The FACS analysis using anti-OMV serum on *E. coli* strains also gave us an indirect result on the ability of the selected antigens to be immunogenic in the context of OMV. Immunization of mice with OMV results in a wide antibody repertoire somehow reflecting what happens during a natural infection with *B. pertussis* or during a vaccination with wP. Clearly, in the density of the OMV lipid bilayer, some abundant proteins might not induce that high antibody response, whereas some less abundant proteins might be immuno-dominant and induce higher responses. While the presence of anti-BrkA, anti-Vag8 and anti-BipA antibodies correlated with high abundance of these proteins on OMV (around ~12%, ~5% and ~3% respectively), the absence of anti-SphB1 and anti-TcfA antibodies was unexpected given the high quantity of these proteins on vesicles (around ~6% and ~4% respectively). Nevertheless, immunization of mice with recombinant proteins could have a completely different outcome and elicit specific anti-adhesive antibodies, as previously demonstrated. Indeed, the protective role of autotransporters is a peculiar trait of *B. pertussis* and thus far, five autotransporters have shown to confer protection in the mouse model (either aerosol or

intranasal challenge) when expressed as recombinant proteins, including Prn (Roberts, Tite et al. 1992), TcfA (Sukumar, Love et al. 2009), SphB1 (de Gouw, de Jonge et al. 2014), Vag8 (de Gouw, de Jonge et al. 2014) and BipA (de Gouw, Serra et al. 2014) suggesting that *B. pertussis* evolved this class of proteins as virulence strategy to colonize the host. Here, we demonstrated that immunization with recombinant BrkA resulted in significant protection against lower respiratory tract infection of *B. pertussis* in the mouse aerosol challenge model. This was different with respect to what previously reported using the mouse intranasal challenge model, where BrkA resulted as an added value only when formulated with aP and not as stand-alone vaccine (Marr, Oliver et al. 2008); however the two studies differ both in the immunization route and in the bacterial infection administration. Finally, we contributed to unravel the mechanism of protection induced by anti-BrkA antibodies showing the inhibitory properties against the bacterial adhesion. In conclusion, BrkA proved to be a promising candidate antigen to improve existing aP vaccines for use in humans. Whether such multi-component aP vaccines that include BrkA and possibly further virulence factors of *B. pertussis* other than Pertussis Toxin, Filamentous Hemagglutinin, Pertactin and Fimbriae have superior efficacy over existing aP vaccines remains to be determined.

Taken together, this study suggests that spontaneously released OMV from *B. pertussis* provide a potential source of protective antigens able to specifically target the colonization step. The inclusion of BrkA and possibly further adhesins may provide a higher protection to current aP vaccines answering to the need of improving the impact of vaccination on the bacterial clearance.

3. Chapter two: contribution of naturally released Outer Membrane Vesicles from *Bordetella pertussis* to bacterial physiology and pathogenesis

Bordetella pertussis has been shown to release OMV both *in vitro* and *in vivo*; these vesicles are widely characterized for their immunogenic and protective properties as vaccine candidates but little information is available about the functional roles of *B. pertussis* OMV during respiratory tract infection (Hozbor, Rodriguez et al. 1999, Roberts, Moreno et al. 2008, Asensio, Gaillard et al. 2011, Bottero, Gaillard et al. 2013, Ormazabal, Bartel et al. 2014, Bottero, Gaillard et al. 2016). Previously, Donato *et al.* showed cell intoxication following OMV treatment and suggested that *B. pertussis* could release OMV as an alternative delivery system for the Adenylate Cyclase Toxin to target cells and increase intracellular cyclic-AMP (Donato, Goldsmith et al. 2012). Nevertheless, the delivery of virulence factors to host cell is just one of the many functions that make OMV an important player in the physiology of Gram-negative bacteria. In this study, we investigated the interaction between purified vesicles and host cells and we were able to show that OMV binding and uptake by different cell lines is strictly related to the bacterial virulent phase and contributes to host cell intoxication. Also, we explored a new putative role for OMV as iron scavengers, reservoirs and delivery systems and proved that they are able to complement *B. pertussis* growth defects in iron-limiting conditions.

3.1. Results and discussion

OMV are naturally released during *B. pertussis* infection of a primary ciliated epithelium

While the release of OMV during *in vitro* growth is largely defined and is a common feature of Gram-negative bacteria, less described is the production of OMV in physiological conditions during the natural infection. Previously, *B. pertussis* organisms with associated OMV were shown through electron microscopy on lung sections from a fatal case of whooping cough. To demonstrate whether OMV are released during the initial phases of *B. pertussis* colonization of the upper respiratory tract we studied the interaction of *B. pertussis* with highly differentiated human bronchial epithelial cells (NHBE cells). These cells, grown at air-liquid interface, express the mucociliary structures typical of the human airways, offering a physiological model to study the early stage of *B. pertussis* infection. Indeed, this model proved to very well reproduce the temporal and spatial stages of adhesion of *B. pertussis* on primary ciliated cells (Guevara, Zhang et al. 2016). NHBE cells were incubated with *B. pertussis* BP536 strain and then analyzed by scanning electron microscopy. As shown in Figure 7, following three days incubation, *B. pertussis* was able to form micro-colonies on ciliated cells and to be associated with large amounts of blebs supporting the hypothesis that OMV could play a role in host-pathogen interaction.

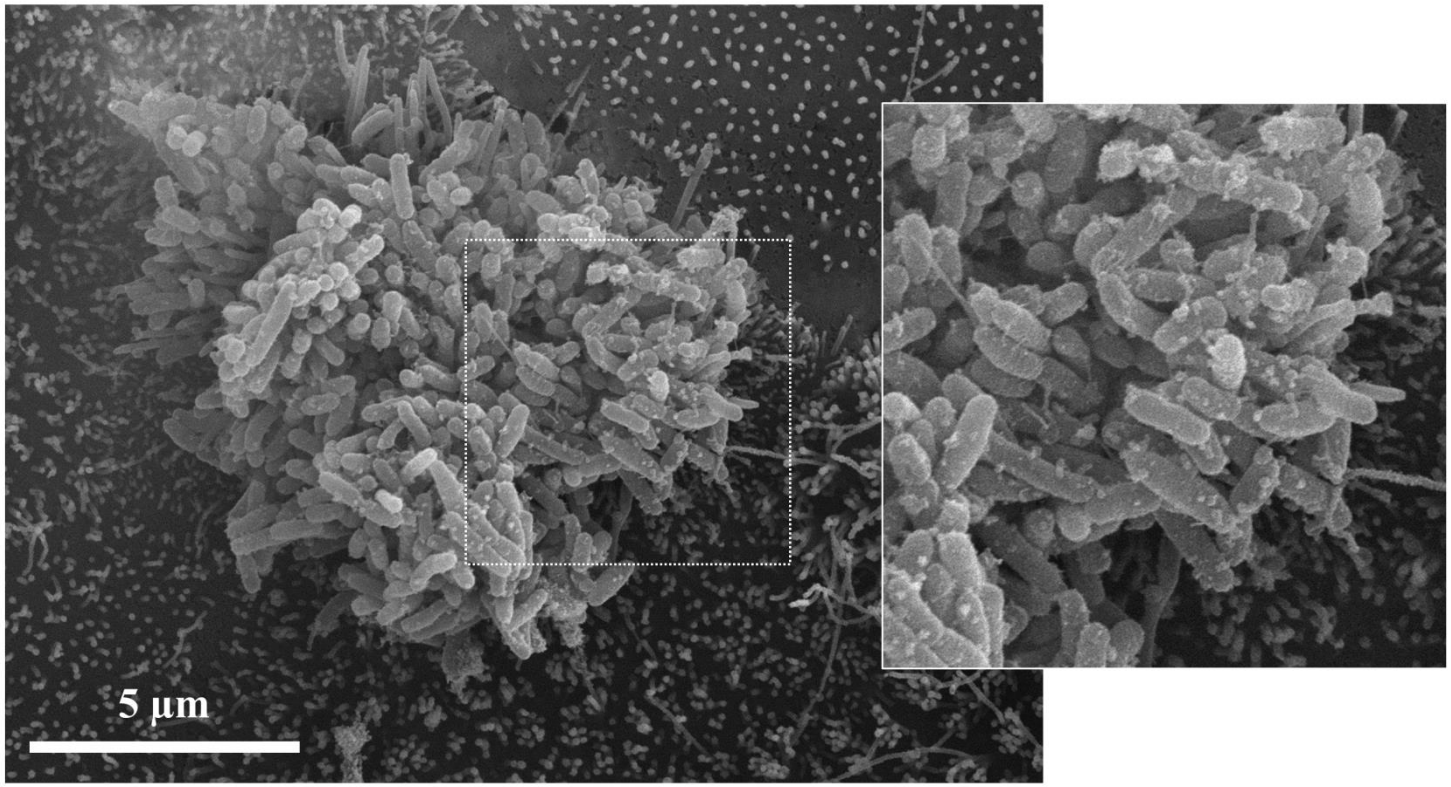

FIG. 7. *Bordetella pertussis* infection of a normal human bronchial epithelium. Scanning electron microscopy of Normal Human Bronchial Epithelial (NHBE) cells differentiated in air-liquid interphase infected with *B. pertussis*. *B. pertussis* is able to form micro-colonies on ciliated cells after three days and releases large amounts of outer membrane vesicles. Dashed box's magnification is reported on the right.

Only OMV released by *B. pertussis* in Bvg+ phase interact with respiratory epithelial cells

In the perspective of studying the interaction of native OMV with host cells, we optimized the protocol for OMV isolation to preserve as much as possible their native features. Different methods for OMV purification from *B. pertussis* bacterial cells or culture supernatant were previously described but these protocols were optimized in a vaccine perspective rather than for functional studies (Hozbor, Rodriguez et al. 1999). For example, the use of detergents like sodium deoxycholate to extract vesicles from bacterial cells or treatment of cell-free culture supernatants with glutaraldehyde results in high yields of OMV but could alter the native conformation of proteins in the vesicles. In the present study, the naturally produced OMV were purified from culture supernatants through ultracentrifugation avoiding any chemical treatment that could alter their intrinsic nature.

Purified OMV were studied for their interaction with host cells. Given that Bvg-activated proteins are mainly associated with colonization and toxicity, OMV were isolated from *B. pertussis* strains BP536 (Bvg+ phase) and BP537 (Bvg- phase) (Decker, James et al. 2012) and analyzed for their ability to bind to A549 and Calu-3 epithelial cells. Cells were incubated with OMV derived from the two Bvg+ and Bvg - strains up to six hours, and analyzed at different time points by immuno-staining and plate reading of OMV-associated fluorescence. As shown in Figure 8A, only Bvg+ OMV were able to bind to A549 cells and Calu-3 cells in a time-dependent manner reaching saturation after 6 hours. The evidence that OMV purified from the avirulent strain BP537 are not able to bind A549 or Calu-3 cells suggests that Bvg-activated virulence factors are responsible for the first attachment of OMV to the membrane of host cells. This in agreement with what known for other pathogens, in which the key

virulence factors are also involved the interaction of bacterial vesicles to host cell (Fiocca, Necchi et al. 1999, Kesty, Mason et al. 2004, Chatterjee and Chaudhuri 2011). To verify whether *B. pertussis* best known adhesins, Filamentous Hemagglutinin (FHA) and Pertactin (69K), had a role in OMV adhesion to epithelial cells, OMV purified from isogenic *B. pertussis* knock-out strains were analyzed for their adhesive properties. As shown in Figure 8B, the adhesive properties of OMV depleted of 69K and FHA were not different from that of OMV derived from the wild-type strain suggesting that this two antigens have no key role in the adhesion of OMV to epithelial cells. This finding was unexpected, considering the primary contribution that has been reported for the two adhesins in the bacterial adhesion on A549 cells (Zanaboni, Arato et al. 2016). Overall these data suggest that bacteria and their vesicles could use different adhesive molecules to interact with epithelial cells and that the differential binding can result in a synergistic rather than a competitive effect during host-pathogen interaction.

Internalization of OMV was qualitatively assessed by confocal and electron microscopy: intracellular localization was mainly perinuclear in A549 cells incubated with OMV for 6 hours and stained with anti-OMV mouse serum (Fig. 9A). In order to better validate the internalization process we decided to employ the more complex and physiological cell model of polarized Calu-3 cells. Indeed, highly polarized epithelial cells are characterized by distinct apical and basolateral plasma membrane domains and by specialized intracellular trafficking machinery which make them more suitable for internalization studies. Interestingly, when polarized Calu-3 cells were analyzed for OMV binding and internalization by electron microscopy, we were able to show that multiple OMV bind and are subsequently internalized in the same intracellular compartment (Fig. 9B).

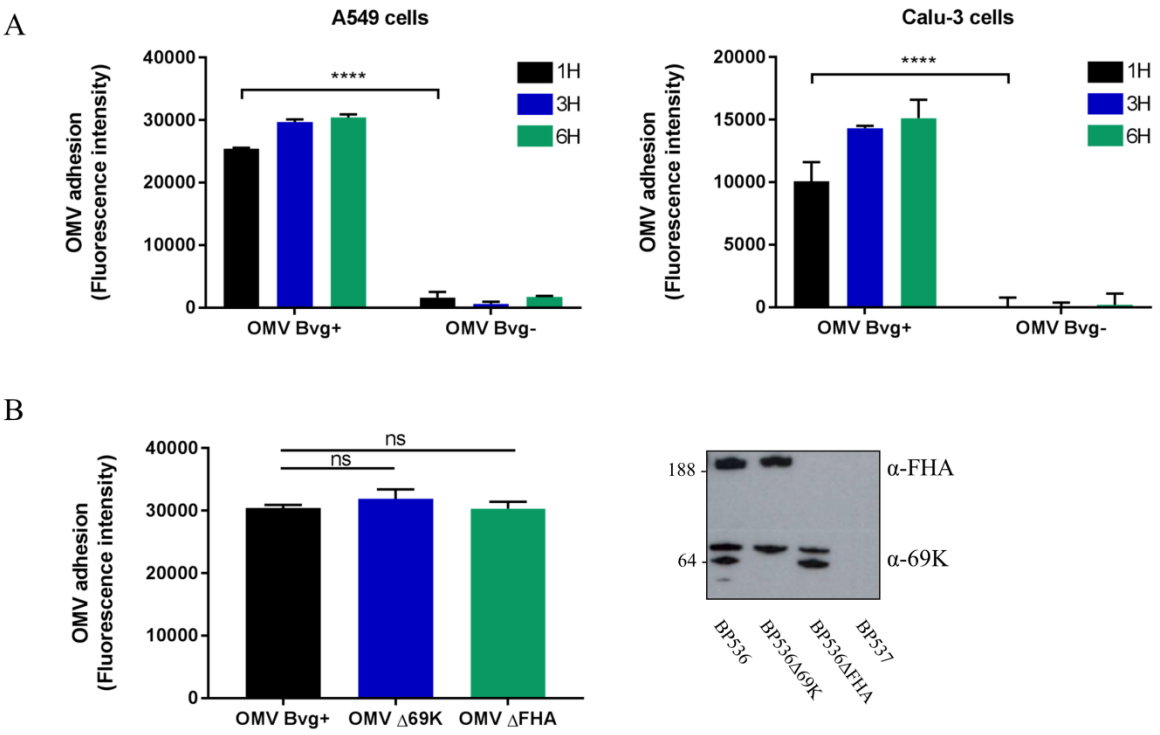

FIG. 8. Interaction between *B. pertussis* OMV and human respiratory epithelial cells. (A) Cells were infected with OMV and, after extensive washes to remove unbound vesicles, cells were fixed and stained with mouse anti-OMV primary antibody and with AlexaFluor488-conjugated anti-mouse secondary antibody. Cell-associated OMV were quantified by fluorescence reading at Ex/Em 485/535 nm. Results represent mean ± SD of one representative of three independent experiments each performed in triplicates, ****=$P < 0.0001$. (B) OMV were purified from *B. pertussis* strain BP536 and from isogenic knock-out strains for FHA and 69K. Cell-associated OMV were quantified by fluorescence reading at Ex/Em 485/535 nm. Results represent mean ± SD of one representative of three independent experiments each performed in triplicates, ns= non-significant. Western blot analyses were performed according to standard procedures. FHA and 69K were identified with polyclonal mouse antisera raised against the purified proteins (diluted 1:1000).

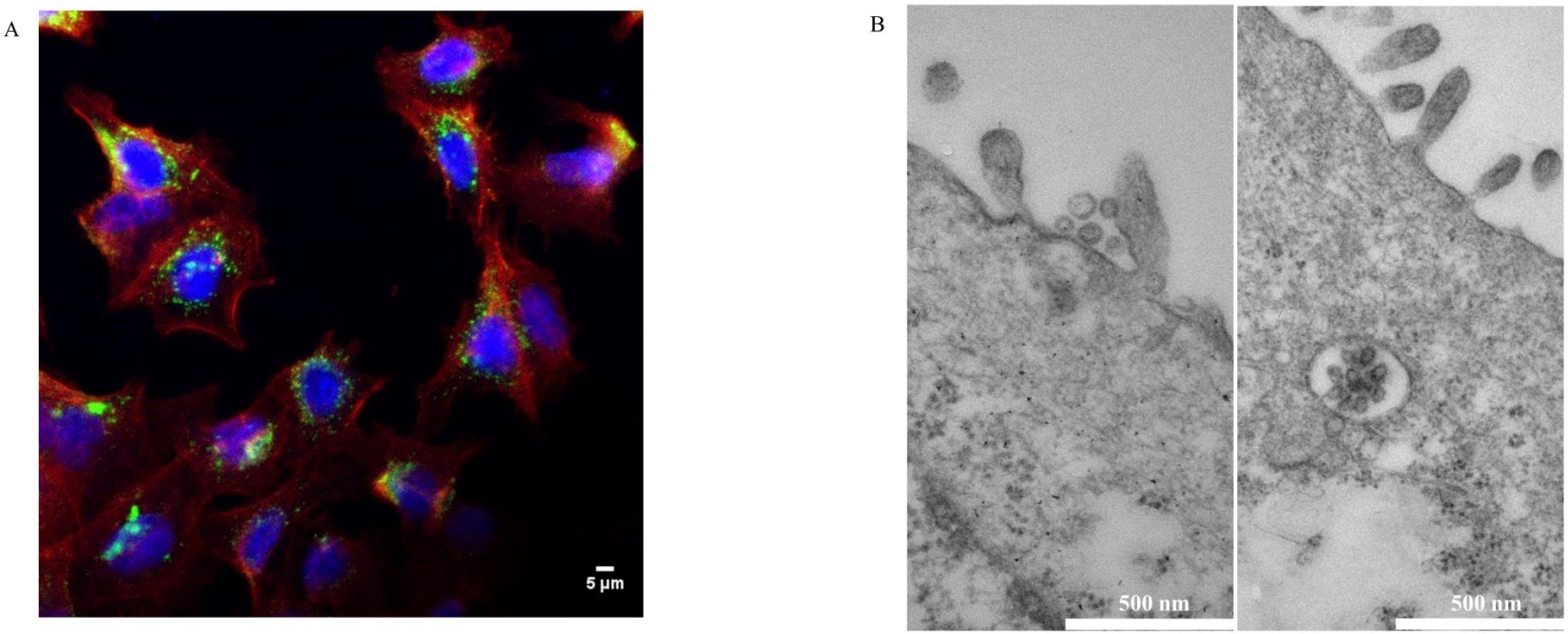

FIG. 9. *B. pertussis* OMV internalization by human respiratory epithelial cells. (A) Confocal microscopy analysis of OMV uptake by A549 cells. A549 cells were incubated with 10 ng/µL of OMV purified from BP536 (Bvg+) and stained with a primary mouse polyclonal anti-OMV serum and secondary fluorescent antibody (green staining). Actin was stained with Phalloidin-568 dye (red staining) and nuclei with DAPI (blue staining). (B) Transmission Electron Microscopy analysis of OMV uptake by polarized Calu-3 cells. Calu-3 cells were incubated with 10 ng/µL of OMV purified from BP536 (Bvg+) then fixed and prepared for TEM analysis.

OMV-associated Pertussis Toxin (PT) is able to promote cell intoxication

We explored whether OMV could contribute to *B. pertussis* pathogenesis by delivering toxins to host cells. Several toxins have been described as associated with OMV (including Cholera Toxin, Heat Labile Enterotoxin, VacA, Shiga Toxin) and they exploit the vesicles as an additional delivery system for cell intoxication processes. We employed a proteomic approach to quantify all the proteins in OMV deriving from bacteria in the virulent phase and we found that Pertussis Toxin was present in OMV, representing about 0.45% of the total protein composition. On the contrary, Adenylate Cyclase Toxin (ACT) and Dermonecrotic Toxin, also known to be secreted, were not present among the OMV components. The absence of ACT in the naturally released vesicles confirmed what already described in two different studies carried-out on OMV purified by ultracentrifugation or ultrafiltration of culture supernatants (Hanawa, Yonezawa et al. 2013, Raeven, van der Maas et al. 2015). These evidences were instead in contrast with what published in previous studies reporting the presence of ACT in OMV (Hozbor, Rodriguez et al. 1999) and cell intoxication detected as cAMP increase attributed to the presence of ACT as OMV cargo (Donato, Goldsmith et al. 2012). These discrepancies are likely imputable to variations in the method employed for OMV isolation; a deoxycholate extraction (Donato, Goldsmith et al. 2012) or a glutaraldehyde treatment (Hozbor, Rodriguez et al. 1999) were performed before ultracentrifugation to increase OMV yields but these chemical agents could alter the native protein composition of the vesicles and favor unwanted membrane-fixing of some proteins.

At first, we confirmed the presence of PT through western blot analysis on OMV (Fig. 10A), including BP536 OMV (a Bvg+ phase strain expressing PT), BP537 OMV (a Bvg- phase strain not expressing PT) and W28 PT9K/129G OMV (a Bvg+ strain

expressing a genetically detoxified PT). Subsequently, to verify the toxicity potential of OMV-associated PT, we tested the ability of the OMV to cause cell clustering in CHO cells. CHO cells were incubated with OMV at concentrations ranging from 160 to 20 μg/ml. As shown in Figure 10B, only OMV derived from a wild-type strain were able to induce CHO cell clustering and the minimal OMV concentration inducing cell intoxication was 40 μg/mL. As expected, OMV from a strain expressing genetically detoxified PT (W28 PT9K/129G) did not show a toxic activity. The active PT in the soluble form was included in the experiment as positive control and the minimal dose needed to cause 100% cell clustering was 2 ng/mL. Although we performed a quantification of the PT associated to OMV by proteomic analysis, the extrapolation of the minimal OMV concentration needed for intoxication remains questionable. The amount of vesicles entering the cells is not predictable and the accessibility or functionality of the PT associated to OMV could differ from its secreted form. These data indicate that the PT packed in OMV is biologically active and could have a synergistic effect with its secreted form during the dissemination to host cells.Whether the presence of PT in the OMV is due to an accumulation in the periplasm or to a re-association through interactions with other outer membrane proteins or LPS remains to be determined. Also, further studies must be conducted to determine the mechanism by which PT is internalized by host cells via OMV and understand the mutual contribution of soluble versus OMV-associated PT during the pathogenesis processes.

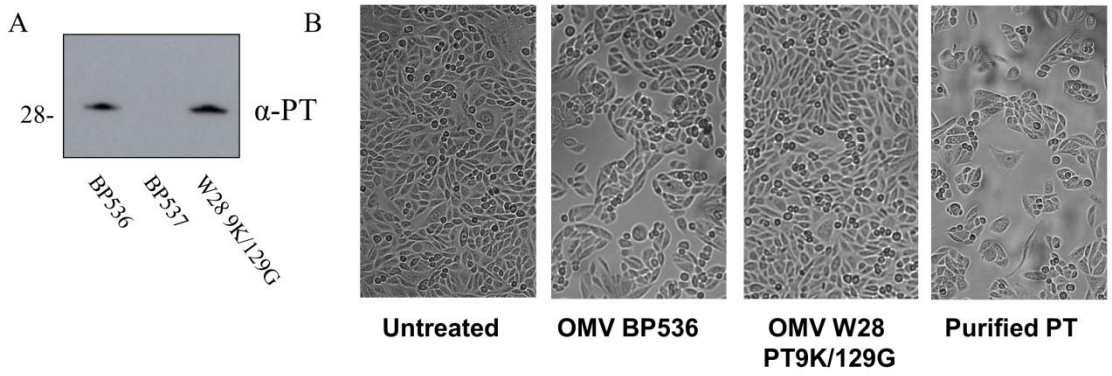

FIG.10. Citotoxicity mediated by OMV-associated PT. A. Presence of PT on OMV. Western blot analyses were performed according to standard procedures. PT was identified with a mouse monoclonal antibody targeting the S1 subunit of the toxin (diluted 1:200). B. CHO cells clustering assay. OMV from BP536 and W28 PT9K/129G (genetically detoxified PT) were added to CHO-K1 cells (2x105cells/ml) and incubated for 16 hours at 37°C in 96-well plates. PT-mediated toxicity was evaluated by observation of morphological alterations (clustered phenotype) by light microscopy. Purified PT (2 ng/mL) was used as positive control. Reported is the treatment with the lowest concentration of OMV inducing cell clustering (40 µg/mL).

OMV have a role in iron delivery

There are growing evidences supporting the role for OMV in the delivery of nutrients of interest to bacterial cells (Evans, Davey et al. 2012, Toledo, Coleman et al. 2012, Biller, Schubotz et al. 2014). In particular, OMV have been described to promote iron acquisition in bacterial communities (Dashper, Hendtlass et al. 2000, Smalley, Byrne et al. 2011, Prados-Rosales, Weinrick et al. 2014). Of interest, a proteomic analysis of *B. pertussis* OMV revealed the presence of a high number of proteins involved in iron uptake and storage (Table 4).

Protein #	Gene #	Gene name
NP_879666	BfrD (BP0856)	TonB-dependent receptor BfrD
NP_881504	BfrG (BP2922)	TonB-dependent receptor BfrG
NP_881648	BP3077	Outer membrane protein
NP_880337	BP1605	Iron binding protein
NP_879667	BfrE (BP0857)	TonB-dependent receptor for iron transport
NP_879314	HemC (BP0456)	Heme receptor

Table 4. Iron receptors and iron binding proteins identified by LC-MS/MS

Clearly, this hypothesis implies that OMV are able to capture iron and deliver it back to the bacteria; thus far, this was demonstrated only for *Mycobacterium tuberculosis* membrane vesicles (Prados-Rosales, Weinrick et al. 2014). We therefore checked if OMV were able to complement the growth defects of *B. pertussis* in iron-limiting conditions (Fig. 11). If no $FeSO_4$ is supplemented in the culture media, *B. pertussis* is still able to grow at slower rate and it reaches stationary phase at a lower optical density. Interestingly, if exogenous OMV, here termed "loaded OMV", were added in the culture media, they were able to restore *B. pertussis* regular growth. This did not occur using OMV purified from *B. pertussis* cultured in the absence of $FeSO_4$ ("empty OMV"). Contrarily to what reported for *M. tuberculosis*, iron starvation does not induce vesicle hyperproduction in *B. pertussis*.

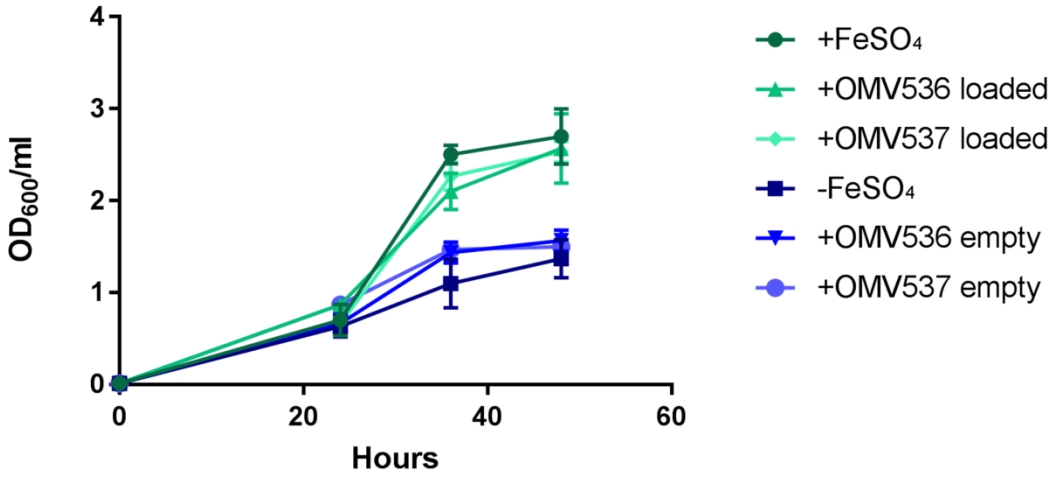

FIG. 11. *B. pertussis* growth under iron-limiting conditions and contribution of OMV to iron delivery. *B. pertussis* strain BP536 was cultured in Steiner-Sholte medium either supplemented or not with $FeSO_4$, in combination with OMV purified from BP536 or BP537 cultures in the presence ("OMV loaded") or absence ("OMV empty") of $FeSO_4$. Error bars represent standard deviations from the means of biological triplicates.

To understand whether OMV were already loaded with iron when released from the bacteria or whether they loaded it after their release in the external milieu, OMV were purified from an iron-limited culture supernatant and were subsequently incubated at 37°C overnight with 10 µg/mL of $FeSO_4$ ("reloaded OMV"). OMV were then purified by ultracentrifugation and washed with D-PBS to remove any excess of $FeSO_4$. As shown in Figure 12, OMV have the intrinsic ability to load iron independently to the presence of bacterial cells; indeed the so termed "reloaded OMV" reacquired the ability to restore *B. pertussis* regular growth in the absence of $FeSO_4$ in the culture media. Opposite to what we observed for the interaction with host cells, this mechanism seemed to be independent of the Bvg regulation; indeed, we obtained comparable results using OMV purified from BP536 or BP537 cultures.

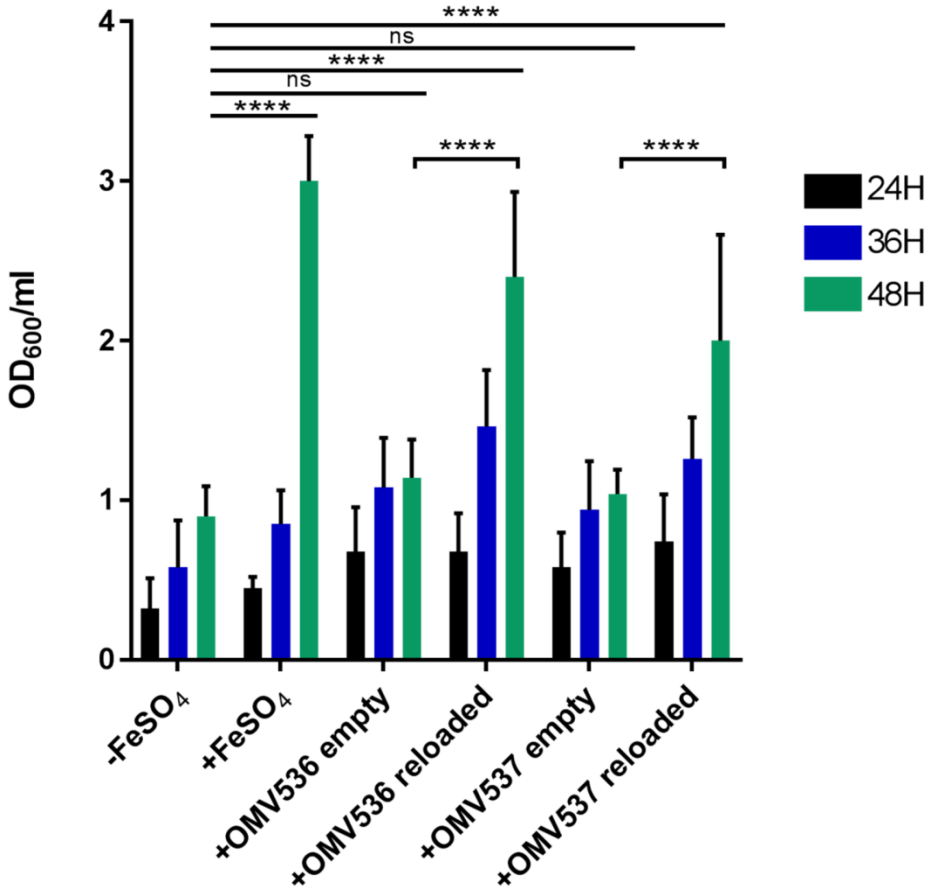

FIG. 12. Iron acquisition by purified *B. pertussis* OMV. *B. pertussis* strain BP536 was cultured in Steiner-Sholte medium either supplemented or not with FeSO4, in combination with OMV purified from BP536 or BP537. Previously, purified OMV were incubated at 37°C overnight either with H_20 ("empty OMV") or with 10 µg/mL of $FeSO_4$ ("reloaded OMV") then washed with D-PBS, ultracentrifuged at 175,000 x g for 2 hours and finally re-suspended in 100µl D-PBS. Error bars represent standard deviations from the means of three biological replicates. ****=P < 0.0001, ns= non-significant.

3.2 Conclusions

In conclusion, our results suggest that the release of outer membrane vesicles from *B. pertussis* is a physio-pathological event that occurs starting from the very early stages of infection of the human respiratory epithelium. Purified vesicles can associate with human lung cells and can be internalized in a time-dependent manner reaching the perinuclear region of the host cells. Many questions remain concerning OMV trafficking and fate after endocytosis and further experiments will be necessary to ultimately identify the host cell and the bacterial factors critical for *B. pertussis* OMV entry. As far as the protein cargo is concerned, PT is the only toxin identified in Bvg+ OMV and it was shown to be functional in the CHO cell clustering assay. Clearly, OMV uptake is not the primary pathway for PT delivery but it may provide an important supplemental mechanism for *B. pertussis* intoxication of host cells and contribute to the inflammatory response during infection, acting synergistically with the all the other secreted toxins. On the other hand, vesicles were shown to function as iron reservoirs and to interact with bacterial cells to deliver the vital metal. Such an involvement of OMV in iron acquisition might be extremely important in the context of infection. Indeed, iron is an essential factor for nearly all organism and bacteria have evolved different mechanisms to obtain it in the host environment. *B. pertussis* was shown to bind to ciliated cells and to form micro-colonies and biofilm while OMV are certainly more readily diffusible and able to cover larger areas. This study lays the basis for the understating of a novel mechanism of *B. pertussis* physio-pathology to be further characterized at the molecular level.

4. Experimental procedures

4.1. Bacterial strains and growth conditions

B. pertussis strains used in this study are reported in Table 5. Bacteria were stored at −80 °C and recovered by plating on Bordet-Gengou (BG) agar plates, supplemented with 15 % sheep blood, for 3 days at 37 °C. Bacteria were then inoculated at initial 600 nm optical density (OD600) of 0.05 in Stainer-Scholte medium supplemented with 0.4 % (w/v) L-cysteine monohydrochloride, 0.1 % (w/v) FeSO4, 0.2 % (w/v) ascorbic acid, 0.04 % (w/v) nicotinic acid, 1 % (w/v) glutathione. Cultures were grown in rotary shakers at 37 °C.

Strain	**Description**	Reference
BP536	BP338 Bvg+; StrepR	(Weiss and Falkow 1983)
BP537	BP536 Bvg-; StrepR	(Relman, Domenighini et al. 1989)
BP-102	BP536 Δ(3.4 kb BamHI-BglII)fhaB; FHA-	(Arico, Nuti et al. 1993)
BP-BBC42	BP536 prn::KanR; PRN-	(Arico, Nuti et al. 1993)
W28 9K/129G	StrepR, genetically detoxified PT	(Pizza, Covacci et al. 1989)

Table 5. Bordetella strains used in this study.

Recombinant DH5α *E. coli* strains were stored at −80 °C, recovered by plating on LB agar plates supplemented with 20 µg/mL chloramphenicol for 16 hours at 37 °C. For liquid cultures, bacteria were inoculated in LB medium supplemented with 20 µg/mL chloramphenicol and were grown in rotary shakers at 37 °C for 16 hours.

4.2. Generation of *E. coli* strains expressing heterologous antigens

E. coli strain DH5α was transformed with a range of 6 plasmids based on the broad host range vector pMMB208 (Morales, Backman et al. 1991) which was modified to express the candidate adhesins. The ApaI-XbaI fragment containing the *lacI* gene and the IPTG-inducible pTac promoter was substituted with an expressing cassette consisting of a constitutive *B. pertussis* promoter and the full length coding sequences for *brkA*, *sphB1*, *vag8*, *tcfA*, *bipA* and *bfrD*. The promoter and the coding sequences were amplified from *B. pertussis* W28 9K/129G genomic DNA using the primers reported in Table 6. The amplified promoter fragment was digested with ApaI/HindIII and the amplified CDS were digested with HindIII/XbaI and were ligated into the ApaI-XbaI digested vector and the final constructs were checked by sequencing. The plasmids were transformed into *E. coli* DH5α and stored at -80 °C.

Primer name	Sequence
pBP0840 Forward	ccc**GGGCCC**TCCTTGAGTGAACTGGGGG
pBP0840 Reverse	ccc**AAGCTT**AATCTCCGTTGATTTGAGTGA
***brkA* Forward**	ccc**AAGCTT**ATGTATCTCGATAGATTCCGTCAA
***brkA* Reverse**	ccc**TCTAGA**TCAGAAGCTGTAGCGGTAGC
***sphB1* Forward**	ccc**AAGCTT**GTGATGCCGCCGCCGGCCGT
***sphB1* Reverse**	ccc**TCTAGA**TCAGTAGCGGTAAGTGAGGCT
***vag8* Forward**	ccc**AAGCTT**ATGGCAGGACAAGCGAGG
***vag8* Reverse**	ccc**TCTAGA**TCACCAGCTGTAGCGATACC
***tcfA* Forward**	ccc**AAGCTT**ATGCACATTTACGGAAATATGAA
***tcfA* Reverse**	ccc**TCTAGA**CTACCAGGCGTAGCGATAGC
***bipA* Forward**	ccc**AAGCTT**ATGAACAAGAACATTTACCGTGTT
***bipA* Reverse**	ccc**TCTAGA**TTAGTAAGGAAAATTGACCGGC
***bfrD* Forward**	ccc**AAGCTT**ATGAAGTTCTACTCTTCCCATCC
***bfrD* Reverse**	ccc**TCTAGA**TCAGTAGCTCAGCTTGAACGTC

Table 6. List of primers used in this study

4.3. Cell lines and growht conditions

The human alveolar epithelial cell line A549 (human lung type II pneumocyte) (ATCC CCL185) was cultured in F12K medium (Invitrogen) supplemented with 10% of fetal bovine serum (FBS), 100 U mL−1 penicillin, and 100 mg mL−1 streptomycin (Sigma) at 37 °C in 5% CO_2. Routine subcultures for A549 pneumocytes were performed at 1:3 split ratios by incubation with 0.05% trypsin-0.02% EDTA for 5 min at 37 °C.

The human airway epithelial cell line Calu-3 (ATCC HTB55) obtained from the metastatic site of lung adenocarcinoma tissue was cultivated in 1:1 DMEM:F12 medium (Invitrogen) supplemented with 10% of fetal bovine serum (FBS), 100 U mL−1 penicillin, and 100 mg mL−1 streptomycin (Sigma) at 37 °C in 5% CO_2. A total of 1×10^6 cm−2 cells were seeded onto polyethylene terephthalate cell culture inserts (Transwell, 1 μm pore size, 12 mm diameter) (BD Bioscience) and were allowed to grow and polarize for 7–10 days. The medium was refreshed every second day. Monolayers reaching transepithelial electrical resistance (TEER) values around 1200 Ω per well, determined using an EVOM TEER meter (World Precision Instruments), were considered fully polarized.

Normal human bronchial epithelial primary cells NHBE (Lonza CC-2540S) isolated from epithelial lining of airways above bifurcation of the lungs were differentiated in air-liquid interphase (ALI) following the provider's instructions. Briefly, cells were cultivated for 3 days in B-ALI™ growth medium. A total of $1{,}5 \times 10^5$ cm−2 cells were seeded onto polyethylene terephthalate cell culture inserts (Transwell, 0,4 μm pore size, 6,5 mm diameter) (Costar) and were allowed to grow with B-ALI™ growth medium both in the basal and apical chamber. After 3 days, B-ALI™ growth medium was removed from the apical chamber and complete B-ALI™ differentiation medium was

added to the basal chamber and changed every second day for 3-4 weeks until cells were completely differentiated.

CHO-K1 cell line (Chinese hamster ovary cells) (ATCC) was cultured in F12K medium (Invitrogen) supplemented with 10% of fetal bovine serum (FBS), 100 U mL−1 penicillin, and 100 mg mL−1 streptomycin (Sigma) at 37 °C in 5% CO_2. Routine subcultures were performed at 1:10 split ratios by incubation with 0.05% trypsin-0.02% EDTA for 5 min at 37 °C.

4.4. OMV isolation

Liquid cultures of BP536 and BP537 were recovered after a 3 days growth in 250 mL baffled flasks. The liquid-air volume ratio resulted critical for OMV production yield and was kept at 1:5 ratio. Bacteria were then pelleted through centrifugation at 5,000 *x g* for 30 minutes. Cell-free supernatants were recovered and filtered through 0.22 μm Stericups filters (Millipore). After ultracentrifugation at 175,000 *x g* for 2 hours, the resulting OMV pellet was washed with Dulbecco's Phosphate-Buffered Saline (D-PBS), further ultracentrifuged at 175,000 *x g* for 2 hours and finally resuspended in 100 μl D-PBS. OMV were quantified through the Lowry assay (DC Protein Assay, BioRad) for total protein content following the manufacturer's instructions.

4.5. SDS-PAGE gel analysis

For sodium dodecyl sulfate-polyacrylamide gel electrophoresis (SDS-PAGE) analysis, ten micrograms of OMV samples were resuspended in 20 mM Tris-HCl (pH 8.0) buffer containing 8% (w/v) SDS and 10 mM DTT, boiled for 5 minutes, separated on NuPAGE™ Novex™ 4-12% Bis-Tris Protein Gels (Invitrogen) and stained with Coomassie Blue R-250.

4.6. Nanoparticle tracking analysis

A NanoSight NS300 instrument (Malvern Ltd) was used to determine OMV particle size and concentration as previously described (Olaya-Abril, Prados-Rosales et al. 2014). Briefly, samples at the protein concentration of 1 μg/μL were diluted 1:500 or 1:1000 in D-PBS and loaded in the sample chamber. Five videos per samples were recorded for 60 seconds and size of individual OMVs and total amount of OMV particles were analyzed by Nanoparticle Tracking Analysis 3.2 software (NanoSight Ltd.). All measurements were performed at room temperature.

4.7. Generation of mouse immune sera

BALB/c mice (10 female/group, 6-week old) (Charles River Laboratories International Inc.) received three intraperitoneal immunizations, with a 4 weeks interval, with aluminum hydroxide adjuvanted OMV from *B. pertussis* strain W28 9K/129G (2.5 μg per dose) or wP vaccine (NIBSC) at one fifteenth of a human dose. Sera were collected before immunization and two weeks after the third immunization. Control mice immunized with adjuvant only were included in the experiments. All animal experiments were performed in compliance with the Italian law with the approval of the local Animal Welfare Body (AWB 2014/06) followed by authorization of Italian Ministry of Health.

4.8. Adhesion assay

A549 cell line (Human epithelial alveolar basal adenocarcinoma, ATCC CCL-185) was maintained in Ham's F-12K medium (Life Technologies) supplemented with 10 % (v/v) heat-inactivated fetal bovine serum (FBS, Gibco) and antibiotics. Cells were grown at 37 °C in humidified atmosphere containing 5 % CO_2. A549 cells were seeded on black 96-well plate ($2.5x10^4$ cells/ well) and cultured for 1 day in absence of antibiotics.

For *E. coli* adhesion assay, bacteria were grown for 16 hours in liquid culture and then washed with D-PBS at 8,000 *x g* for 5 minutes and resuspended at OD_{600} 0.1 in F12-K medium. One hundred microliters were transferred in triplicates on plated A549 cells. Infected cells were incubated for 3 hours at 37 °C. After extensive washing to remove unbound bacteria, cells were fixed with 3.7 % (v/v) formaldehyde (Sigma) for 20 minutes, blocked with D-PBS containing 3% (w/v) Bovine Serum Albumin (BSA) for 15 minutes and incubated with rabbit anti-*Escherichia coli* polyclonal antibodies diluted in D-PBS + 1 % (w/v) BSA (1:500) for 1 hour. After washes, samples were incubated with Alexa Fluor® 488 goat anti-rabbit IgG (1:500) (Molecular Probes) for 30 minutes. After three washes with D-PBS, fluorescence was measured at excitation/emission 485/535 nm by Tecan Infinite F200PRO microplate reader. For OMV adhesion assay, vesicles were re-suspended in D-PBS to the final concentration of 10 ng/μL and 100 μL were transferred in triplicates on plated A549 cells. After 6 hours of incubation, cells were washed extensively with D-PBS, then fixed with 3.7 % (v/v) formaldehyde (Sigma) for 20 minutes, blocked with D-PBS containing 3% (w/v) BSA for 15 minutes and incubated with mouse anti-OMV serum diluted in D-PBS + 1 % (w/v) BSA (1:5000) for 1 hour. After washes, samples were incubated with Alexa Fluor® 488 rabbit anti-mouse IgG (1:500) (Molecular Probes) for 30 minutes. After

three washes with D-PBS, fluorescence was measured at excitation/emission 485/535 nm by Tecan Infinite F200PRO microplate reader. Adhesion assays were performed 3 times on different days; statistical analyses were performed using unpaired t test (for *B. pertussis* OMV adhesion) and one-way ANOVA with Dunnett's multiple comparison test (for *E. coli* adhesion).

4.9. Adhesion inhibition assay

For *B. pertussis* adhesion inhibition assay, bacteria were grown for 16 hours in liquid culture and then pelleted at 8,000 ×*g* for 5 min and resuspended in D-PBS at OD_{600} 0.5. A volume of 445 µL of bacterial suspension was then mixed with 50 µL of 1 M $NaHCO_3$ and 5 µL of Alexa Fluor® 488 Carboxylic Acid, Succinimidyl Ester (Molecular Probes, Life Technologies) and incubated for 15 minutes at 37 °C. After centrifugation at 8,000 *x g* for 5 minutes at room temperature, supernatant was removed and pellet was washed once with 1 mL PBS to remove unbound dye and bacteria were finally resuspended in F12-K medium at OD_{600} 0.2. Pooled mouse sera were four-fold serially diluted in F-12K medium containing 1 % (v/v) naïve mouse serum and pre-incubated with labeled *B. pertussis* for 1 hour at 37 °C in 1:1 ratio. One hundred microliters of bacteria/serum mixtures were transferred in triplicates on plated A549 cells. Infected cells were incubated for 1 hour at 37 °C. After extensive washing to remove unbound bacteria, fluorescence was measured at excitation/emission 485/535 nm by Tecan Infinite F200PRO microplate reader. For *E. coli* adhesion inhibition assay, we used the same protocol used for *B. pertussis* adhesion inhibition assay, but we revealed *E. coli* adhering bacteria by immuno-fluorescence using rabbit anti-*Escherichia coli* polyclonal antibodies as previously described for the adhesion assay.

4.10. Proteomic analysis by LC-MS/MS, data analysis and bioinformatics

For quantitative proteomic analysis, one hundred micrograms of OMV were TCA precipitated as previously described (Tani, Stella et al. 2014) and the protein pellet was resuspended in 50 mM ammonium bicarbonate containing 0.1% (w/v) RapiGest SF™ (Waters) and 5 mM DTT and heated at 100 °C for 10 minutes. Digestions were performed overnight at 37 °C with 2.5 μg trypsin (Promega). Digestions were stopped with 0.1% (v/v) final formic acid, desalted using OASIS HLB cartridges (Waters) as described by the manufacturer, dried in a Centrivap Concentrator (Labconco) and resuspended in 50 μl of 3% (v/v) ACN and 0.1% (v/v) formic acid. Peptide mixtures were stored at −20 °C until further analysis. An Acquity HPLC instrument (Waters) was coupled on-line to a Q Exactive Plus (Thermo Fisher Scientific) with an electrospray ion source (Thermo Fisher Scientific). The peptide mixture (10 μg) was loaded onto a C18-reversed phase column Acquity UPLC peptide CSH C18 130Å, 1.7μm 1 x 150 mm and separated with a linear gradient of 28–85% buffer B (0.1% (v/v) formic acid in ACN) at a flow rate of 50 μL/min and 50 °C. MS data was acquired in positive mode using a data-dependent acquisition (DDA) dynamically choosing the five most abundant precursor ions from the survey scan (300–1600 *m/z*) at 70,000 resolution for HCD fragmentation. Automatic Gain Control (AGC) was set at $3E^{+6}$. For MS/MS acquisition, the isolation of precursors was performed with a 3 *m/z* window and MS/MS scans were acquired at a resolution of 17,500 at 200 *m/z* with normalized collision energy of 26 eV.

Three technical replicates were performed on two biological replicates of OMV purified from Bvg+ and Bvg- strains. The mass spectrometric raw data were analyzed with the PEAKS software ver. 8 (Bioinformatics Solutions Inc.) for de novo sequencing,

database matching identification and label free quantification. Peptide scoring for identification was based on a database search with an initial allowed mass deviation of the precursor ion of up to 15 ppm. The allowed fragment mass deviation was 0.05 Da. Protein identification from MS/MS spectra was performed against *B. pertussis* Tohama I protein database (3,436 protein entries) combined with common contaminants (human keratins and autoproteolytic fragments of trypsin) with a FDR set at 0.1%. Enzyme specificity was set as C-terminal to Arg and Lys, without allowing cleavage at proline bonds and a maximum of four missed cleavages. N-terminal pyroGlu, Met oxidation and Gln/Asn deamidation were set as variable modifications. Tryptic digestion from rabbit phosphorylase B (Waters) was used as internal standard for label free quantification (2 pmol/μL) using a mass tolerance of 20 ppm, a retention time shift tolerance of 2 min, minimum 3 different peptides with a FDR set at 0.1%.

The percentage for each protein in the total samples was subsequently calculated multiplying the theoretical molecular weight (MW) of each protein by the average peak area and then dividing by the sum of all the average peak areas in each sample, multiplied by their theoretical molecular weigth (Average area*MW/Sum(Average area*MW)). Percentages were averaged between the two biological samples and finally, the fold increase of each protein amount in Bvg+ vs. Bvg- and in Bvg- vs. Bvg+ was calculated. A 10-fold increase in amount was set as a threshold for defining Bvg phase specificity of each protein.

PSORTb version 3.0.2 was used for the prediction of protein cellular compartment (http://www.psort.org/psortb/) (Nakai and Horton 1999). Further refinement was performed for lipoprotein annotation that were sorted from unknown identifications using the precompiled genome annotation by DOLOP (http://www.mrc-lmb.cam.ac.uk/genomes/dolop/) (Madan Babu and Sankaran 2002).

4.11. Flow citometry

E. coli strains were grown for 16 hours in liquid culture. Bacteria were then pelleted and washed with D-PBS at 8,000 *x g* for 5 minutes. Bacteria were then blocked with D-PBS containing 3% (w/v) BSA (Sigma) for 15 minutes and incubated with mouse anti-OMV serum diluted in D-PBS + 1% (w/v) BSA (1:500) for 1 hour. After washes, samples were incubated with Alexa Fluor® 488 goat anti-mouse IgG (1:500) (Molecular Probes) for 30 minutes. Finally, bacteria were fixed with 3.7% (v/v) formaldehyde (Sigma) for 20 minutes and flow cytometry analysis was performed using FACS Canto II flow cytometer (BD Biosciences).

4.12. Recombinant antigen production

The gene fragment encoding BrkA, corresponding to protein residues 43-726, was amplified by PCR from *B. pertussis* W28 9K/129G genomic DNA. The PCR fragment was cloned into the pET15-TEV vector, a modified version of the pET15 vector (Novagen), constructed to express N-terminal His-tagged (TEV cleavable) proteins (Klock, Koesema et al. 2008). Protein expression was performed in *E. coli* BL21 (DE3) cells, by using EnPresso B growth systems (BioSilta) supplemented with 100 μg/mL ampicillin. Bacteria were grown at 30°C for 12 hours, and recombinant protein expression was then induced by the addition of 1 mM isopropyl β-D-1-thiogalactopyranoside (IPTG) at 25°C for additional 24 hours. Proteins were extracted from the insoluble fraction with 6 M of guanidinium chloride and then purified by immobilized metal ion affinity chromatography (IMAC) using HiTRAP in 8 M Urea, 100 mM NaH_2PO_4 (pH 8) 10 mM Tris HCl (pH 8), 500 mM imidazole (GE Healthcare Life Sciences) and refolded by multistep dialysis in 50 mM NaH_2PO_4 (pH 7.5), 300 mM NaCl, 1% (v/v) glycerol.

4.13. Mouse aerosol challenge model

BALB/c mice (10 female/group, 6-week old) (Charles River Laboratories International Inc.) received three intraperitoneal immunizations, with a 4 weeks interval, with aluminum hydroxide adjuvanted recombinant BrkA (10 μg per dose) or with adjuvant only. A bacterial suspension of BP536 from a 24-hour culture was generated at 2×10^9 CFU/mL in D-PBS with 1% (w/v) casein salts (Sigma). BrkA-vaccinated and control mice were placed in a closed chamber in which the bacterial suspension was administered as an aerosol for 10 min using a nebulizer device with an administration rate of 0.5 mL/min. *B. pertussis* infection was monitored by performing colony forming units (CFU) counts on lungs from groups of 10 mice seven days after aerosol challenge. Lungs were aseptically removed and homogenized in 2 mL of sterile physiological saline buffer with 1% (w/v) casein salts on ice. Ten microliters of undiluted homogenate or of serially diluted homogenates were spotted in triplicate onto Bordet-Gengou agar plates, and the number of CFU was estimated after three days of incubation at 37°C. Statistical analysis was performed using unpaired t test (Mann-Whitney test).

4.14. Electron microscopy

B. pertussis strain BP536 was grown for 16 hours at 37°C. An aliquot corresponding to OD600=2 was then pelleted, washed with Dulbecco's Phosphate-Buffered Saline (D-PBS) and re-suspended in 1 mL B-ALI™ growth medium without antibiotics. 100 μL were then used to infect NHBE cells grown on transwell inserts. After 1 hour of infection, cells were washed with D-PBS to remove unbound bacteria and left in ALI for three days before proceeding with the preparation of the samples for electron microscopy.

Calu-3 cells were incubated with OMV purified from *B. pertussis* strain BP536 liquid cultures, re-suspended in D-PBS at the final concentration of 10 ng/µL. After 6 hour of incubation, cells were washed with D-PBS to remove unbound OMV before proceeding with the preparation of the samples for electron microscopy.

Samples were fixed O/N at 4°C in sodium cacodylate buffer 0,1M containing 2,5% glutaraldehyde and 2.5% formaldehyde and then post-fixed in 1% OsO4. Samples were then dried by the critical point method using CO2 in a Balzers Union CPD 020. For SEM samples were sputter-coated with gold in a Balzers MED 010 unit. For TEM, the dried samples were embedded in LRWhite resin and stained with uranyl acetate and lead citrate.

4.15. Confocal microscopy

For immunofluorescence confocal microscopy analysis, A549 cells (4×10^4/well) were seeded on 8-well chamber slides (BD BioCoat) and cultured for two days. Cells were then incubated with 10 ng/µL of OMV (diluted in F12K + 1% FBS) for 6 hours at 37°C. After washing with D-PBS to remove unbound OMV, cells were fixed with 3.7% (v/v) formaldehyde (Sigma), permeabilized using Triton 0.25% for 10 minutes at room temperature and blocked with D-PBS containing 3% (w/v) BSA for 15 minutes. Cells were then incubated with mouse anti-OMV serum diluted in D-PBS + 1 % (w/v) BSA (1:5000) for 1 hour. After washes, samples were incubated with Alexa Fluor® 488 rabbit anti-mouse IgG (1:500) (Molecular Probes) in combination with Alexa Fluor 568 Phalloidin for 30 minutes. After three washes with D-PBS, glass coverslips were mounted with ProLong® reagent with DAPI (Life Technologies) and analyzed using a Zeiss LSM710 confocal microscope.

4.16. Western Blotting

OMV were resuspended in SDS-containing sample loading buffer, boiled for 5 minutes, separated by SDS-PAGE using the NuPAGE Gel System (Invitrogen) and transferred onto nitrocellulose membranes for Western blot analysis. Western blots were performed according to standard procedures. FHA and 69K were identified with polyclonal mouse antisera raised against the purified proteins (diluted 1:1000). PT subunit 1 (S1) was identified with a mouse monoclonal antibody (diluted 1:200). In all cases, an anti-mouse antiserum conjugated to horseradish peroxidase (Dako) was used as the secondary antibody (1:5000). Bands were visualized with Super Signal West Pico Chemiluminescent Substrate (Pierce) following the manufacturer's instructions.

4.17. PT intoxication assay

PT toxicity test was performed following the principles described previously (Hewlett, Sauer et al. 1983). Two-fold serially diluted OMV from BP536 and W28 PT9K/129G (genetically detoxified PT) were mixed with CHO-K1 cells ($2x10^5$cells/ml) and incubated for 16 hours at 37°C in 96-well plates. PT-mediated toxicity was evaluated by observation of morphological alterations (clustered phenotype) by light microscopy. Purified PT at 2 ng/ml was used as positive control.

4.18. Growth assay for iron delivery

A frozen stock of *B. pertussis* strain BP536 was inoculated onto BG agar plates. An aliquot was taken to inoculate 2 mL of Steiner Sholte medium (supplemented without $FeSO_4$) to an initial OD at 600 nm of 0.05. The cultures were incubated at 37°C with shaking. $FeSO_4$ or OMV were added at the final concentration of 10 μg/mL and 5 ng/μL

respectively. OMV were either purified from *B. pertussis* cultures in the presence of $FeSO_4$ ("loaded OMV"), in the absence of $FeSO_4$ ("empty OMV"), or in the absence of $FeSO_4$ and subsequently incubated with $FeSO_4$ ("reloaded OMV"). Cell growth was monitored by measuring the OD at 600 nm. Growth assays were performed 3 times on different days; statistical analyses were performed using two-way ANOVA with Dunnett's multiple comparison test.

5. Bibliography

- Alaniz, R. C., B. L. Deatherage, J. C. Lara and B. T. Cookson (2007). "Membrane vesicles are immunogenic facsimiles of Salmonella typhimurium that potently activate dendritic cells, prime B and T cell responses, and stimulate protective immunity in vivo." J Immunol **179**(11): 7692-7701.
- Arico, B., J. F. Miller, C. Roy, S. Stibitz, D. Monack, S. Falkow, R. Gross and R. Rappuoli (1989). "Sequences required for expression of Bordetella pertussis virulence factors share homology with prokaryotic signal transduction proteins." Proc Natl Acad Sci U S A **86**(17): 6671-6675.
- Arico, B., S. Nuti, V. Scarlato and R. Rappuoli (1993). "Adhesion of Bordetella pertussis to eukaryotic cells requires a time-dependent export and maturation of filamentous hemagglutinin." Proc Natl Acad Sci U S A **90**(19): 9204-9208.
- Asensio, C. J., M. E. Gaillard, G. Moreno, D. Bottero, E. Zurita, M. Rumbo, P. van der Ley, A. van der Ark and D. Hozbor (2011). "Outer membrane vesicles obtained from Bordetella pertussis Tohama expressing the lipid A deacylase PagL as a novel acellular vaccine candidate." Vaccine **29**(8): 1649-1656.
- Ausiello, C. M. and A. Cassone (2014). "Acellular pertussis vaccines and pertussis resurgence: revise or replace?" MBio **5**(3): e01339-01314.
- Barkin, R. M. and M. E. Pichichero (1979). "Diphtheria-pertussis-tetanus vaccine: reactogenicity of commercial products." Pediatrics **63**(2): 256-260.
- Beveridge, T. J. (1999). "Structures of gram-negative cell walls and their derived membrane vesicles." J Bacteriol **181**(16): 4725-4733.
- Beveridge, T. J., S. A. Makin, J. L. Kadurugamuwa and Z. Li (1997). "Interactions between biofilms and the environment." FEMS Microbiol Rev **20**(3-4): 291-303.

- Biller, S. J., F. Schubotz, S. E. Roggensack, A. W. Thompson, R. E. Summons and S. W. Chisholm (2014). "Bacterial vesicles in marine ecosystems." Science **343**(6167): 183-186.
- Bisgard, K. M., F. B. Pascual, K. R. Ehresmann, C. A. Miller, C. Cianfrini, C. E. Jennings, C. A. Rebmann, J. Gabel, S. L. Schauer and S. M. Lett (2004). "Infant pertussis: who was the source?" Pediatr Infect Dis J **23**(11): 985-989.
- Black, R. E., S. Cousens, H. L. Johnson, J. E. Lawn, I. Rudan, D. G. Bassani, P. Jha, H. Campbell, C. F. Walker, R. Cibulskis, T. Eisele, L. Liu, C. Mathers, W. H. O. Child Health Epidemiology Reference Group of and Unicef (2010). "Global, regional, and national causes of child mortality in 2008: a systematic analysis." Lancet **375**(9730): 1969-1987.
- Bottero, D., M. E. Gaillard, A. Errea, G. Moreno, E. Zurita, L. Pianciola, M. Rumbo and D. Hozbor (2013). "Outer membrane vesicles derived from Bordetella parapertussis as an acellular vaccine against Bordetella parapertussis and Bordetella pertussis infection." Vaccine **31**(45): 5262-5268.
- Bottero, D., M. E. Gaillard, E. Zurita, G. Moreno, D. S. Martinez, E. Bartel, S. Bravo, F. Carriquiriborde, A. Errea, C. Castuma, M. Rumbo and D. Hozbor (2016). "Characterization of the immune response induced by pertussis OMVs-based vaccine." Vaccine **34**(28): 3303-3309.
- Braun, V. and H. Wolff (1975). "Attachment of lipoprotein to murein (peptidoglycan) of Escherichia coli in the presence and absence of penicillin FL 1060." J Bacteriol **123**(3): 888-897.
- Brickman, T. J., R. J. Suhadolc and S. K. Armstrong (2015). "Interspecies variations in Bordetella catecholamine receptor gene regulation and function." Infect Immun **83**(12): 4639-4652.

- Cascales, E., A. Bernadac, M. Gavioli, J. C. Lazzaroni and R. Lloubes (2002). "Pal lipoprotein of Escherichia coli plays a major role in outer membrane integrity." J Bacteriol **184**(3): 754-759.
- Chatterjee, D. and K. Chaudhuri (2011). "Association of cholera toxin with Vibrio cholerae outer membrane vesicles which are internalized by human intestinal epithelial cells." FEBS Lett **585**(9): 1357-1362.
- Cherry, J. D. (1999). "Pertussis in the preantibiotic and prevaccine era, with emphasis on adult pertussis." Clin Infect Dis **28 Suppl 2**: S107-111.
- Chiappini, E., A. Stival, L. Galli and M. de Martino (2013). "Pertussis re-emergence in the post-vaccination era." BMC Infect Dis **13**: 151.
- Christie, C. D. and R. S. Baltimore (1989). "Pertussis in neonates." Am J Dis Child **143**(10): 1199-1202.
- Clark, T. A., N. E. Messonnier and S. C. Hadler (2012). "Pertussis control: time for something new?" Trends Microbiol **20**(5): 211-213.
- Cornia, P. B., A. L. Hersh, B. A. Lipsky, T. B. Newman and R. Gonzales (2010). "Does this coughing adolescent or adult patient have pertussis?" JAMA **304**(8): 890-896.
- Cotter, P. A. and A. M. Jones (2003). "Phosphorelay control of virulence gene expression in Bordetella." Trends Microbiol **11**(8): 367-373.
- Coutte, L., S. Alonso, N. Reveneau, E. Willery, B. Quatannens, C. Locht and F. Jacob-Dubuisson (2003). "Role of adhesin release for mucosal colonization by a bacterial pathogen." J Exp Med **197**(6): 735-742.
- Dashper, S. G., A. Hendtlass, N. Slakeski, C. Jackson, K. J. Cross, L. Brownfield, R. Hamilton, I. Barr and E. C. Reynolds (2000). "Characterization

of a novel outer membrane hemin-binding protein of Porphyromonas gingivalis." J Bacteriol **182**(22): 6456-6462.

- de Gouw, D., M. I. de Jonge, P. W. Hermans, H. J. Wessels, A. Zomer, A. Berends, C. Pratt, G. A. Berbers, F. R. Mooi and D. A. Diavatopoulos (2014). "Proteomics-identified Bvg-activated autotransporters protect against bordetella pertussis in a mouse model." PLoS One **9**(8): e105011.
- de Gouw, D., D. A. Diavatopoulos, H. J. Bootsma, P. W. Hermans and F. R. Mooi (2011). "Pertussis: a matter of immune modulation." FEMS Microbiol Rev **35**(3): 441-474.
- de Gouw, D., P. W. Hermans, H. J. Bootsma, A. Zomer, K. Heuvelman, D. A. Diavatopoulos and F. R. Mooi (2014). "Differentially expressed genes in Bordetella pertussis strains belonging to a lineage which recently spread globally." PLoS One **9**(1): e84523.
- de Gouw, D., D. O. Serra, M. I. de Jonge, P. W. Hermans, H. J. Wessels, A. Zomer, O. M. Yantorno, D. A. Diavatopoulos and F. R. Mooi (2014). "The vaccine potential of Bordetella pertussis biofilm-derived membrane proteins." Emerg Microbes Infect **3**(8): e58.
- Decker, K. B., T. D. James, S. Stibitz and D. M. Hinton (2012). "The Bordetella pertussis model of exquisite gene control by the global transcription factor BvgA." Microbiology **158**(Pt 7): 1665-1676.
- Deora, R., H. J. Bootsma, J. F. Miller and P. A. Cotter (2001). "Diversity in the Bordetella virulence regulon: transcriptional control of a Bvg-intermediate phase gene." Mol Microbiol **40**(3): 669-683.
- Donato, G. M., C. S. Goldsmith, C. D. Paddock, J. C. Eby, M. C. Gray and E. L. Hewlett (2012). "Delivery of Bordetella pertussis adenylate cyclase toxin to target cells via outer membrane vesicles." FEBS Lett **586**(4): 459-465.

- Dorward, D. W., C. F. Garon and R. C. Judd (1989). "Export and intercellular transfer of DNA via membrane blebs of Neisseria gonorrhoeae." J Bacteriol **171**(5): 2499-2505.
- Elder, K. D. and E. T. Harvill (2004). "Strain-dependent role of BrkA during Bordetella pertussis infection of the murine respiratory tract." Infect Immun **72**(10): 5919-5924.
- Evans, A. G., H. M. Davey, A. Cookson, H. Currinn, G. Cooke-Fox, P. J. Stanczyk and D. E. Whitworth (2012). "Predatory activity of Myxococcus xanthus outer-membrane vesicles and properties of their hydrolase cargo." Microbiology **158**(Pt 11): 2742-2752.
- Fan, E., N. Chauhan, D. B. Udatha, J. C. Leo and D. Linke (2016). "Type V Secretion Systems in Bacteria." Microbiol Spectr **4**(1).
- Fernandez, R. C. and A. A. Weiss (1994). "Cloning and sequencing of a Bordetella pertussis serum resistance locus." Infect Immun **62**(11): 4727-4738.
- Finn, T. M. and D. F. Amsbaugh (1998). "Vag8, a Bordetella pertussis bvg-regulated protein." Infect Immun **66**(8): 3985-3989.
- Finn, T. M. and L. A. Stevens (1995). "Tracheal colonization factor: a Bordetella pertussis secreted virulence determinant." Mol Microbiol **16**(4): 625-634.
- Fiocca, R., V. Necchi, P. Sommi, V. Ricci, J. Telford, T. L. Cover and E. Solcia (1999). "Release of Helicobacter pylori vacuolating cytotoxin by both a specific secretion pathway and budding of outer membrane vesicles. Uptake of released toxin and vesicles by gastric epithelium." J Pathol **188**(2): 220-226.
- Guevara, C., C. Zhang, J. A. Gaddy, J. Iqbal, J. Guerra, D. P. Greenberg, M. D. Decker, N. Carbonetti, T. D. Starner, P. B. McCray, Jr., F. R. Mooi and O. G.

Gomez-Duarte (2016). "Highly differentiated human airway epithelial cells: a model to study host cell-parasite interactions in pertussis." Infect Dis (Lond) **48**(3): 177-188.

- Hanawa, T., H. Yonezawa, H. Kawakami, S. Kamiya and S. K. Armstrong (2013). "Role of Bordetella pertussis RseA in the cell envelope stress response and adenylate cyclase toxin release." Pathog Dis **69**(1): 7-20.
- Haurat, M. F., W. Elhenawy and M. F. Feldman (2015). "Prokaryotic membrane vesicles: new insights on biogenesis and biological roles." Biol Chem **396**(2): 95-109.
- Hellman, J., P. M. Loiselle, E. M. Zanzot, J. E. Allaire, M. M. Tehan, L. A. Boyle, J. T. Kurnick and H. S. Warren (2000). "Release of gram-negative outer-membrane proteins into human serum and septic rat blood and their interactions with immunoglobulin in antiserum to Escherichia coli J5." J Infect Dis **181**(3): 1034-1043.
- Hewlett, E. L., K. T. Sauer, G. A. Myers, J. L. Cowell and R. L. Guerrant (1983). "Induction of a novel morphological response in Chinese hamster ovary cells by pertussis toxin." Infect Immun **40**(3): 1198-1203.
- Higgs, R., S. C. Higgins, P. J. Ross and K. H. Mills (2012). "Immunity to the respiratory pathogen Bordetella pertussis." Mucosal Immunol **5**(5): 485-500.
- Hozbor, D., M. E. Rodriguez, J. Fernandez, A. Lagares, N. Guiso and O. Yantorno (1999). "Release of outer membrane vesicles from Bordetella pertussis." Curr Microbiol **38**(5): 273-278.
- Kesty, N. C., K. M. Mason, M. Reedy, S. E. Miller and M. J. Kuehn (2004). "Enterotoxigenic Escherichia coli vesicles target toxin delivery into mammalian cells." EMBO J **23**(23): 4538-4549.

- Klein, N. P., J. Bartlett, A. Rowhani-Rahbar, B. Fireman and R. Baxter (2012). "Waning protection after fifth dose of acellular pertussis vaccine in children." N Engl J Med **367**(11): 1012-1019.
- Klock, H. E., E. J. Koesema, M. W. Knuth and S. A. Lesley (2008). "Combining the polymerase incomplete primer extension method for cloning and mutagenesis with microscreening to accelerate structural genomics efforts." Proteins **71**(2): 982-994.
- Lacey, B. W. (1960). "Antigenic modulation of Bordetella pertussis." J Hyg (Lond) **58**: 57-93.
- Madan Babu, M. and K. Sankaran (2002). "DOLOP--database of bacterial lipoproteins." Bioinformatics **18**(4): 641-643.
- Mallory, F. B. and A. A. Hornor (1912). "Pertussis: The histological Lesion in the Respiratory Tract." J Med Res **27**(2): 115-124 113.
- Manning, A. J. and M. J. Kuehn (2011). "Contribution of bacterial outer membrane vesicles to innate bacterial defense." BMC Microbiol **11**: 258.
- Marr, N., D. C. Oliver, V. Laurent, J. Poolman, P. Denoel and R. C. Fernandez (2008). "Protective activity of the Bordetella pertussis BrkA autotransporter in the murine lung colonization model." Vaccine **26**(34): 4306-4311.
- Marr, N., N. R. Shah, R. Lee, E. J. Kim and R. C. Fernandez (2011). "Bordetella pertussis autotransporter Vag8 binds human C1 esterase inhibitor and confers serum resistance." PLoS One **6**(6): e20585.
- Mashburn-Warren, L., J. Howe, K. Brandenburg and M. Whiteley (2009). "Structural requirements of the Pseudomonas quinolone signal for membrane vesicle stimulation." J Bacteriol **191**(10): 3411-3414.

- Mattoo, S. and J. D. Cherry (2005). "Molecular pathogenesis, epidemiology, and clinical manifestations of respiratory infections due to Bordetella pertussis and other Bordetella subspecies." Clin Microbiol Rev **18**(2): 326-382.
- McBroom, A. J., A. P. Johnson, S. Vemulapalli and M. J. Kuehn (2006). "Outer membrane vesicle production by Escherichia coli is independent of membrane instability." J Bacteriol **188**(15): 5385-5392.
- McBroom, A. J. and M. J. Kuehn (2007). "Release of outer membrane vesicles by Gram-negative bacteria is a novel envelope stress response." Mol Microbiol **63**(2): 545-558.
- Melton, A. R. and A. A. Weiss (1993). "Characterization of environmental regulators of Bordetella pertussis." Infect Immun **61**(3): 807-815.
- Melvin, J. A., E. V. Scheller, J. F. Miller and P. A. Cotter (2014). "Bordetella pertussis pathogenesis: current and future challenges." Nat Rev Microbiol **12**(4): 274-288.
- Merkel, T. J., C. Barros and S. Stibitz (1998). "Characterization of the bvgR locus of Bordetella pertussis." J Bacteriol **180**(7): 1682-1690.
- Merkel, T. J., S. Stibitz, J. M. Keith, M. Leef and R. Shahin (1998). "Contribution of regulation by the bvg locus to respiratory infection of mice by Bordetella pertussis." Infect Immun **66**(9): 4367-4373.
- Mills, K. H., P. J. Ross, A. C. Allen and M. M. Wilk (2014). "Do we need a new vaccine to control the re-emergence of pertussis?" Trends Microbiol **22**(2): 49-52.
- Mooi, F. R., N. A. Van Der Maas and H. E. De Melker (2014). "Pertussis resurgence: waning immunity and pathogen adaptation - two sides of the same coin." Epidemiol Infect **142**(4): 685-694.

- Morales, V. M., A. Backman and M. Bagdasarian (1991). "A series of wide-host-range low-copy-number vectors that allow direct screening for recombinants." Gene **97**(1): 39-47.
- Nakai, K. and P. Horton (1999). "PSORT: a program for detecting sorting signals in proteins and predicting their subcellular localization." Trends Biochem Sci **24**(1): 34-36.
- Olaya-Abril, A., R. Prados-Rosales, M. J. McConnell, R. Martin-Pena, J. A. Gonzalez-Reyes, I. Jimenez-Munguia, L. Gomez-Gascon, J. Fernandez, J. L. Luque-Garcia, C. Garcia-Lidon, H. Estevez, J. Pachon, I. Obando, A. Casadevall, L. A. Pirofski and M. J. Rodriguez-Ortega (2014). "Characterization of protective extracellular membrane-derived vesicles produced by Streptococcus pneumoniae." J Proteomics **106**: 46-60.
- Ormazabal, M., E. Bartel, M. E. Gaillard, D. Bottero, A. Errea, M. E. Zurita, G. Moreno, M. Rumbo, C. Castuma, D. Flores, M. J. Martin and D. Hozbor (2014). "Characterization of the key antigenic components of pertussis vaccine based on outer membrane vesicles." Vaccine **32**(46): 6084-6090.
- Paddock, C. D., G. N. Sanden, J. D. Cherry, A. A. Gal, C. Langston, K. M. Tatti, K. H. Wu, C. S. Goldsmith, P. W. Greer, J. L. Montague, M. T. Eliason, R. C. Holman, J. Guarner, W. J. Shieh and S. R. Zaki (2008). "Pathology and pathogenesis of fatal Bordetella pertussis infection in infants." Clin Infect Dis **47**(3): 328-338.
- Pizza, M., A. Covacci, A. Bartoloni, M. Perugini, L. Nencioni, M. T. De Magistris, L. Villa, D. Nucci, R. Manetti, M. Bugnoli and et al. (1989). "Mutants of pertussis toxin suitable for vaccine development." Science **246**(4929): 497-500.

- Postels-Multani, S., H. J. Schmitt, C. H. Wirsing von Konig, H. L. Bock and H. Bogaerts (1995). "Symptoms and complications of pertussis in adults." Infection **23**(3): 139-142.
- Prados-Rosales, R., B. C. Weinrick, D. G. Pique, W. R. Jacobs, Jr., A. Casadevall and G. M. Rodriguez (2014). "Role for Mycobacterium tuberculosis membrane vesicles in iron acquisition." J Bacteriol **196**(6): 1250-1256.
- Raeven, R. H., L. van der Maas, W. Tilstra, J. P. Uittenbogaard, T. H. Bindels, B. Kuipers, A. van der Ark, J. L. Pennings, E. van Riet, W. Jiskoot, G. F. Kersten and B. Metz (2015). "Immunoproteomic Profiling of Bordetella pertussis Outer Membrane Vesicle Vaccine Reveals Broad and Balanced Humoral Immunogenicity." J Proteome Res **14**(7): 2929-2942.
- Relman, D. A., M. Domenighini, E. Tuomanen, R. Rappuoli and S. Falkow (1989). "Filamentous hemagglutinin of Bordetella pertussis: nucleotide sequence and crucial role in adherence." Proc Natl Acad Sci U S A **86**(8): 2637-2641.
- Roberts, M., J. P. Tite, N. F. Fairweather, G. Dougan and I. G. Charles (1992). "Recombinant P.69/pertactin: immunogenicity and protection of mice against Bordetella pertussis infection." Vaccine **10**(1): 43-48.
- Roberts, R., G. Moreno, D. Bottero, M. E. Gaillard, M. Fingermann, A. Graieb, M. Rumbo and D. Hozbor (2008). "Outer membrane vesicles as acellular vaccine against pertussis." Vaccine **26**(36): 4639-4646.
- Ross, P. J., C. E. Sutton, S. Higgins, A. C. Allen, K. Walsh, A. Misiak, E. C. Lavelle, R. M. McLoughlin and K. H. Mills (2013). "Relative contribution of Th1 and Th17 cells in adaptive immunity to Bordetella pertussis: towards the rational design of an improved acellular pertussis vaccine." PLoS Pathog **9**(4): e1003264.

- Schwechheimer, C. and M. J. Kuehn (2015). "Outer-membrane vesicles from Gram-negative bacteria: biogenesis and functions." Nat Rev Microbiol **13**(10): 605-619.
- Smalley, J. W., D. P. Byrne, A. J. Birss, H. Wojtowicz, A. Sroka, J. Potempa and T. Olczak (2011). "HmuY haemophore and gingipain proteases constitute a unique syntrophic system of haem acquisition by Porphyromonas gingivalis." PLoS One **6**(2): e17182.
- Stockbauer, K. E., B. Fuchslocher, J. F. Miller and P. A. Cotter (2001). "Identification and characterization of BipA, a Bordetella Bvg-intermediate phase protein." Mol Microbiol **39**(1): 65-78.
- Sukumar, N., C. F. Love, M. S. Conover, N. D. Kock, P. Dubey and R. Deora (2009). "Active and passive immunizations with Bordetella colonization factor A protect mice against respiratory challenge with Bordetella bronchiseptica." Infect Immun **77**(2): 885-895.
- Tani, C., M. Stella, D. Donnarumma, M. Biagini, P. Parente, A. Vadi, C. Magagnoli, P. Costantino, F. Rigat and N. Norais (2014). "Quantification by LC-MS(E) of outer membrane vesicle proteins of the Bexsero(R) vaccine." Vaccine **32**(11): 1273-1279.
- Toledo, A., J. L. Coleman, C. J. Kuhlow, J. T. Crowley and J. L. Benach (2012). "The enolase of Borrelia burgdorferi is a plasminogen receptor released in outer membrane vesicles." Infect Immun **80**(1): 359-368.
- Tozzi, A. E., L. P. Celentano, M. L. Ciofi degli Atti and S. Salmaso (2005). "Diagnosis and management of pertussis." CMAJ **172**(4): 509-515.
- Tuomanen, E. I. and J. O. Hendley (1983). "Adherence of Bordetella pertussis to human respiratory epithelial cells." J Infect Dis **148**(1): 125-130.

- Uhl, M. A. and J. F. Miller (1996). "Integration of multiple domains in a two-component sensor protein: the Bordetella pertussis BvgAS phosphorelay." EMBO J **15**(5): 1028-1036.
- Vergara-Irigaray, N., A. Chavarri-Martinez, J. Rodriguez-Cuesta, J. F. Miller, P. A. Cotter and G. Martinez de Tejada (2005). "Evaluation of the role of the Bvg intermediate phase in Bordetella pertussis during experimental respiratory infection." Infect Immun **73**(2): 748-760.
- Warfel, J. M., J. Beren, V. K. Kelly, G. Lee and T. J. Merkel (2012). "Nonhuman primate model of pertussis." Infect Immun **80**(4): 1530-1536.
- Warfel, J. M., L. I. Zimmerman and T. J. Merkel (2014). "Acellular pertussis vaccines protect against disease but fail to prevent infection and transmission in a nonhuman primate model." Proc Natl Acad Sci U S A **111**(2): 787-792.
- Weiss, A. A. and S. Falkow (1983). "Transposon insertion and subsequent donor formation promoted by Tn501 in Bordetella pertussis." J Bacteriol **153**(1): 304-309.
- Wendelboe, A. M., E. Njamkepo, A. Bourillon, D. D. Floret, J. Gaudelus, M. Gerber, E. Grimprel, D. Greenberg, S. Halperin, J. Liese, F. Munoz-Rivas, R. Teyssou, N. Guiso, A. Van Rie and G. Infant Pertussis Study (2007). "Transmission of Bordetella pertussis to young infants." Pediatr Infect Dis J **26**(4): 293-299.
- Wendelboe, A. M., A. Van Rie, S. Salmaso and J. A. Englund (2005). "Duration of immunity against pertussis after natural infection or vaccination." Pediatr Infect Dis J **24**(5 Suppl): S58-61.

- Xing, D., K. Markey, R. G. Das and I. Feavers (2014). "Whole-cell pertussis vaccine potency assays: the Kendrick test and alternative assays." Expert Rev Vaccines **13**(10): 1175-1182.
- Zanaboni, E., V. Arato, M. Pizza, A. Seubert and R. Leuzzi (2016). "A novel high-throughput assay to quantify the vaccine-induced inhibition of Bordetella pertussis adhesion to airway epithelia." BMC Microbiol **16**: 215.